# CHAPTER IV

# RESULTS AND DISCUSSION

In this research, poly[acrylamide-*co*-(acrylic acid)] hydrogels, poly[AM-*co*-(AA)], were prepared by free radical polymerization in aqueous solutions of acrylamide and acrylic acid using the *N, N'*- methylenebisacrylamide (N-MBA), ammonium persulphate (APS) and *N, N, N', N'*-tetramethylethylenediamine (TEMED) as crosslinking agent, initiator and co-initiator, respectively.

From the previous work, the foaming agent had been generally used in the superabsorbent polymers synthesis to achieve the higher water absorbency [39]. However, the polymeric flocculants for treating the wastewater were often synthesized without the foaming agent [26, 40] because the water absorbency was not the main objective in this application. Thus, in this research, poly[acrylamide-*co*-(acrylic acid)] and polymeric flocculant were synthesized by chemical crosslinking polymerization without a foaming agent.

For the preparation of poly[AM-*co*-(AA)], the monomer was each dissolved in water, then the crosslinking agent, initiator and co-initiator were added into the monomeric solution to initiate the free radical crosslinking copolymerization.

During the polymerization, N-MBA molecules can be incorporated with two chains of acrylamide and acrylic acid simultaneously and formed a chemical crosslink between them. As a result, the poly[AM-*co*-(AA)] grows into a three dimensional network as shown in Scheme 4.1 [41, 42]. The polymerization took place for an hour to achieve the poly[AM-*co*-(AA)] hydrogel which was a colorless and soft elastic gel.

In the case of polymeric flocculant of aluminium hydroxide-poly[acrylamide-*co*-(acrylic acid)] (AHAMAAs), they were synthesized by free radical polymerization using aluminium hydroxide as a coagulant in the presence of acrylamide and acrylic acid as a comonomer pair. *N, N'*- methylenebisacrylamide (N-MBA), ammonium persulphate (APS) and *N, N, N', N'*-tetramethylethylenediamine (TEMED) as crosslinking agent, initiator and co-initiator, respectively. The step of gel formation was similar to poly[AM-*co*-(AA)] but the elastic gel after the polymerization was cloudy caused by the presence of aluminium hydroxide. Scheme 4.1 presents the synthesis of poly[AM-*co*-(AA)] by free radical crosslinking copolymerization as follows.

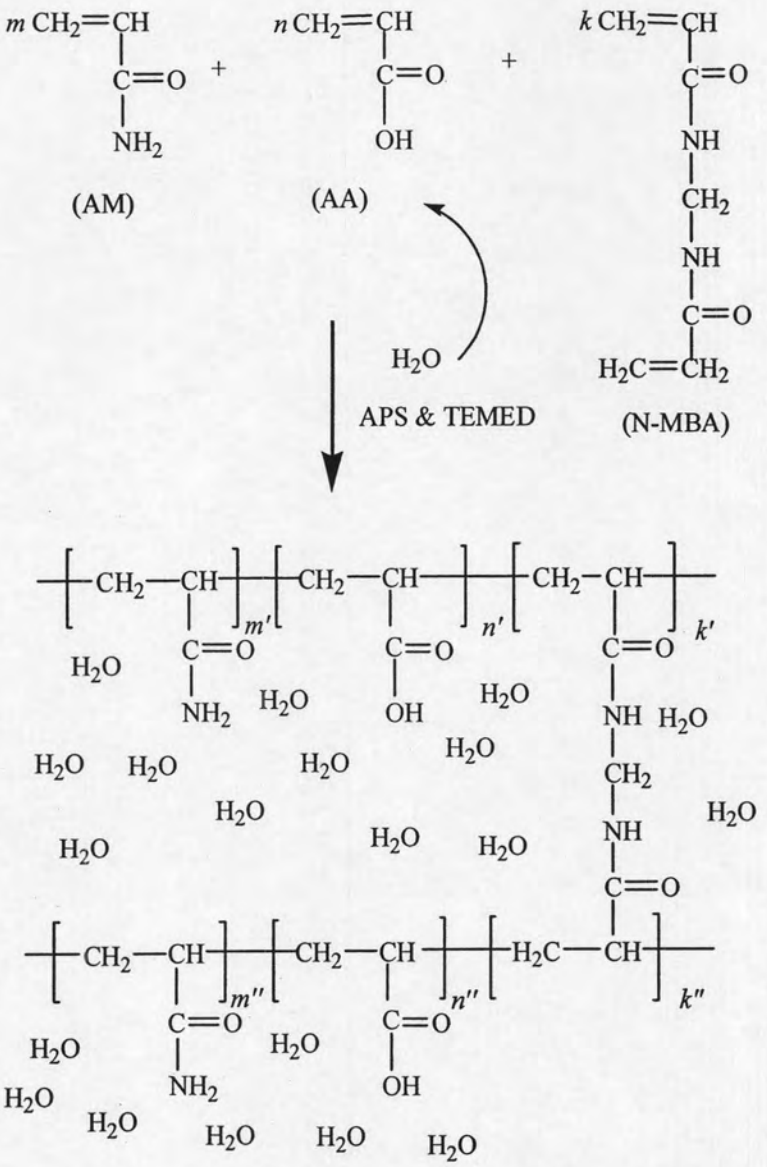


**Scheme 4.1** Synthesis of poly[AM-*co*-(AA)] by free radical copolymerization [42].

## 4.1 Characterization

### 4.1.1 FTIR spectra of the synthesized $Al(OH)_3$, poly[AM-*co*-(AA)] and AHAMAA

The functional groups of $Al(OH)_3$, poly[AM-*co*-(AA)] and AHAMAA were characterized by Fourier Transform Infrared Spectroscopy. The spectra were shown in Figures 4.1-4.3 and the assignments were shown in Tables 4.1-4.3.

From the $Al(OH)_3$-FTIR spectrum in Figure 4.1, it shows the peak of O-H stretching which indicates the presence of the hydroxide group. In addition, it also shows the peak of Al-OH and O-Al at 980 and 618 $cm^{-1}$, respectively [40]. This result confirms that the hydrolysis product of aluminium sulphate is aluminium hydroxide and the peak of sulphate group was found at 1129 and 1653 $cm^{-1}$, resulting from aluminium sulphate residue contaminated in $Al(OH)_3$ [43].

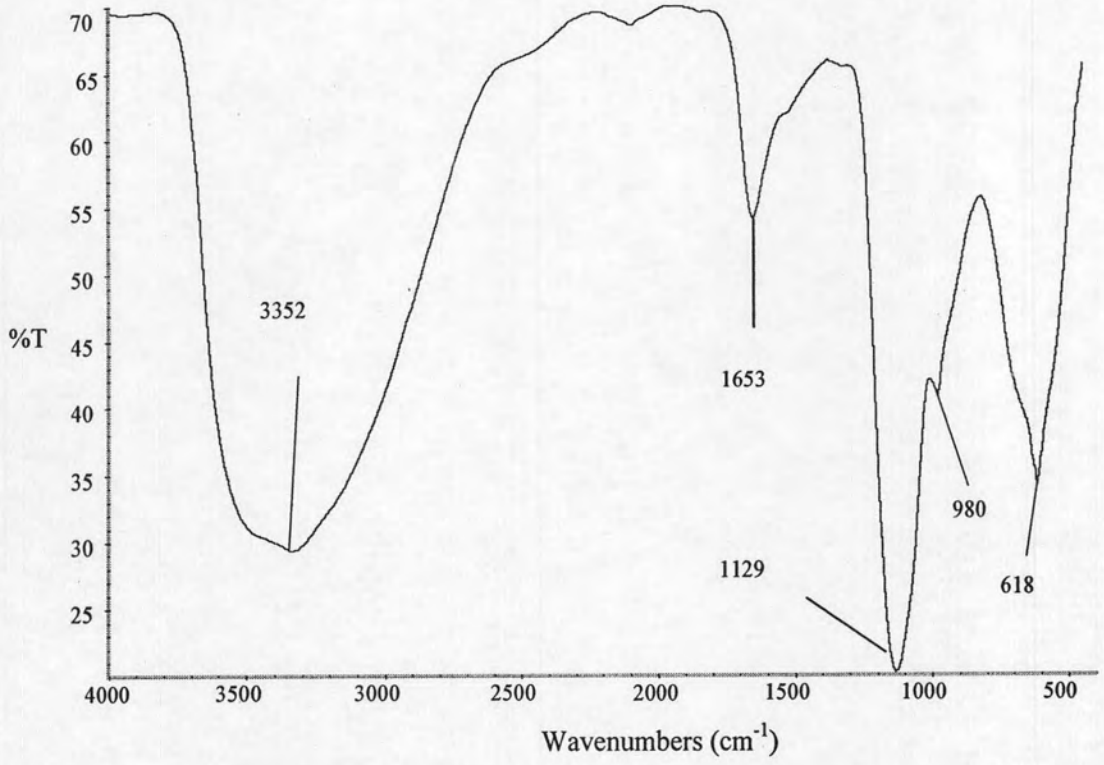


**Figure 4.1** FTIR spectrum of $Al(OH)_3$

**Table 4.1** Assignments for FTIR spectrum of $Al(OH)_3$

| Wave number ($cm^{-1}$) | Assignments |
|---|---|
| 3352 | O-H stretching |
| 1653, 1129 | S=O stretching of sulfate group |
| 980 | Al-OH |
| 618 | O-Al |

From Figure 4.2, FTIR spectrum of poly[AM-*co*-(AA)] confirms the presence of the carboxyl (3440 and 1638 $cm^{-1}$) and carboxamide functional groups (3291 and 1350 $cm^{-1}$) in the copolymer [40].

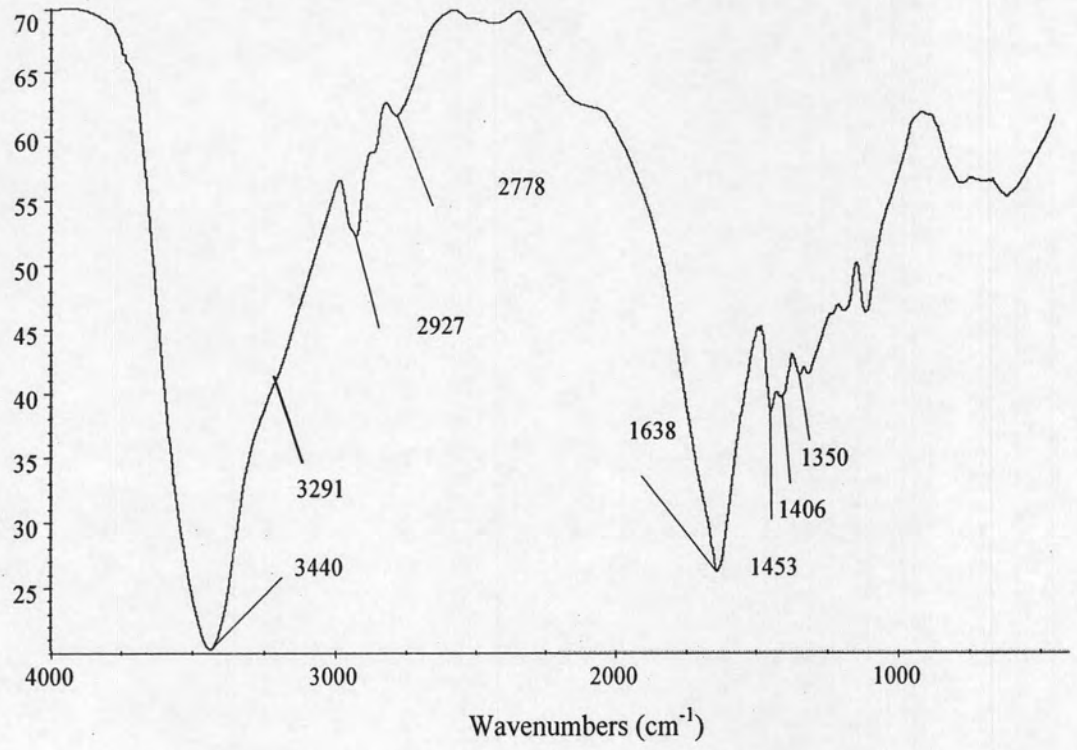


**Figure 4.2** FTIR spectrum of poly[AM-*co*-(AA)]

**Table 4.2** Assignments for FTIR spectrum of poly[AM-*co*-(AA)]

| Wave number ($cm^{-1}$) | Assignments |
|---|---|
| 3440 | O-H stretching of acid |
| 3291 | N-H stretching of amide |
| 2927, 2778 | C-H stretching of CH, $CH_2$ |
| 1638 | C=O stretching of acid |
| 1453, 1406 | C-H bending of CH, $CH_2$ |
| 1350 | C-N stretching of amide |

From the FTIR spectrum of AHAMAA in Figure 4.3, it shows the coordination of carboxylate anion and the metal ion (aluminium ion) at the peak of 1658 $cm^{-1}$ which indicates the complex formation of the copolymer and $Al(OH)_3$ [40].

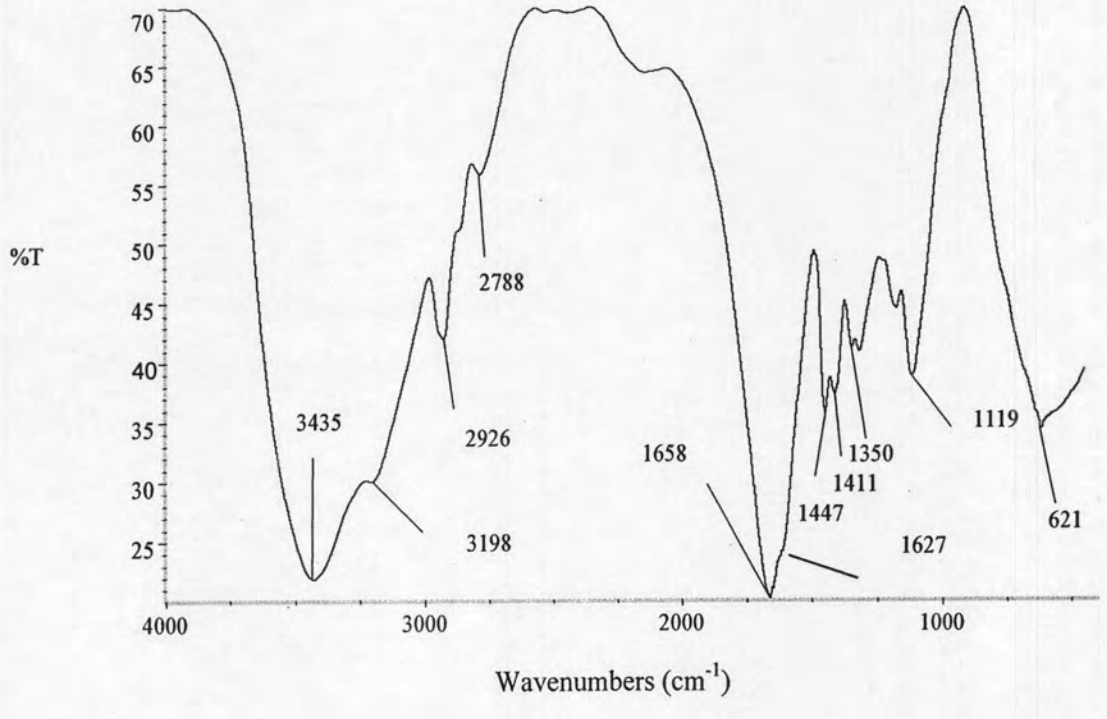


**Figure 4.3** FTIR spectrum of AHAMAA

**Table 4.3** Assignments for FTIR spectrum of AHAMAA

| Wave number ($cm^{-1}$) | Assignments |
|---|---|
| 3435 | O-H stretching of acid |
| 3199 | N-H stretching of amide |
| 2927, 2788 | C-H stretching of CH, $CH_2$ |
| 1658 | the coordination of carboxylate anion and the metal ion [40] |
| 1627 | C=O stretching of acid |
| 1447, 1411 | C-H bending of CH, $CH_2$ |
| 1350 | C-N stretching of amide |
| 621 | O-Al |

### 4.1.2 Characterization of $Al(OH)_3$ and AHAMAA by $^{27}$Al-NMR

The $^{27}$Al-NMR spectra of aluminium form in $Al(OH)_3$ and AHAMAA characterized by $^{27}$Al nuclear magnetic resonance spectrometer are shown in Figure 4.4.

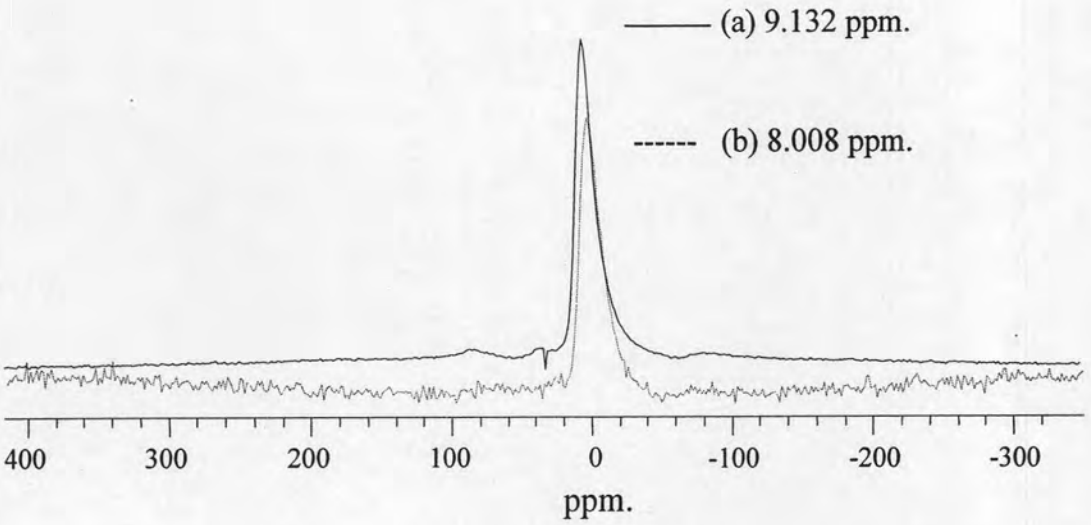


**Figure 4.4** The $^{27}$Al-NMR of (a) $Al(OH)_3$ and (b) AHAMAA synthesized with $4x10^{-3}$ mol AA, $2.3x10^{-4}$ mol N-MBA, $1.6x10^{-4}$ mol APS and $12x10^{-4}$ mol TEMED

In generally, $Al(OH)_3$ from a hydrolysis can form Al in the form of monomeric, dimeric, polymeric species ($Al_{13}$) and $Al(OH)^{4-}$. The signal near the 0.0 ppm represents the monomeric and dimeric species, the signal at 62.5 ppm denotes the $Al_{13}$ species, and the signal at 80.0 ppm indicates the formation of $Al(OH)^{4-}$ [29]. From Figure 4.4, there is only one signal each at 9.132 and 8.008 ppm for $Al(OH)_3$ and AHAMAA, respectively, which indicates that $Al(OH)_3$ and Al in AHAMAA are the monomeric and/ or dimeric species.

### 4.1.3 Morphology of copolymer and copolymer complex by scanning electron microscopy

4.1.3.1 Surface morphology of poly[AM-*co*-(AA)] and AHAMAA

The poly[AM-*co*-(AA)] and AHAMAA characterized by scanning electron microscopy (SEM) show the surface morphology in Figures 4.5 and 4.6.

From Figure 4.5, the SEM micrograph of poly[AM-*co*-(AA)] shows two different appearances of surface, i.e., a smooth surface in Figure 4.5 (a) and a porous surface in Figure 4.5 (b). The porous surface could be resulted from the crosslinking reaction between two acrylamide chains to form the cyclic imide functional group [40]. For the SEM micrograph of AHAMAA in Figure 4.6, the surface of AHAMAA was different from that of the poly[AM-*co*-(AA)] because AHAMAA had also the white powder particles on the smooth surface.

4.1.3.2 The distribution of aluminium element in the AHAMAA

The distribution of carbon and aluminium elements on the surface of AHAMAA was detected by energy dispersive X-ray spectrometer (EDX). From Figure 4.7, it shows the similar distribution of carbon and aluminium elements on the AHAMAA surfaces. However, the percentage of carbon elements was 38.42, which was higher than that of aluminium element (0.46%). The presence of aluminium element could influence greatly the water absorbency to be investigated in Section 4.3.

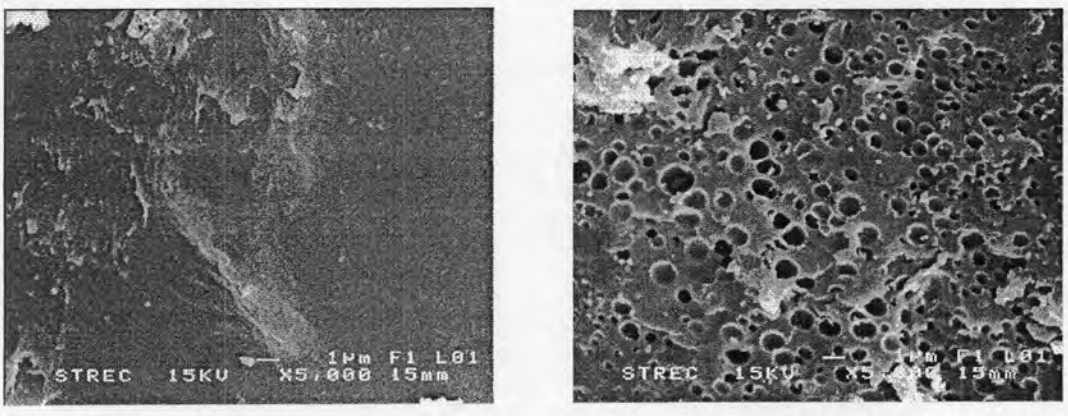


**(a)** **(b)**

**Figure 4.5** SEM micrographs of poly[AM-*co*-(AA)] prepared with $4x10^{-3}$ mol AA, $2.3x10^{-4}$ mol N-MBA, $1.6x10^{-4}$ mol APS and $12x10^{-4}$ mol TEMED at two areas

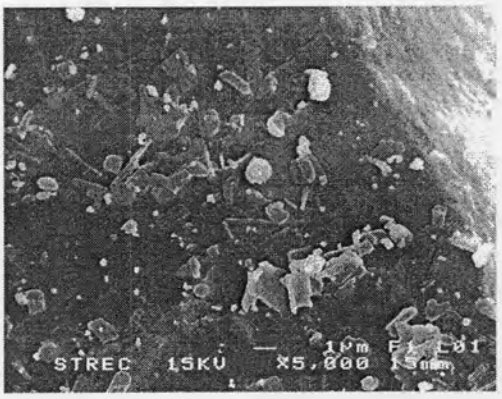


**Figure 4.6** SEM micrograph of AHAMAA prepared with $4x10^{-3}$ mol AA, $2.3x10^{-4}$ mol N-MBA, $1.6x10^{-4}$ mol APS and $12x10^{-4}$ mol TEMED

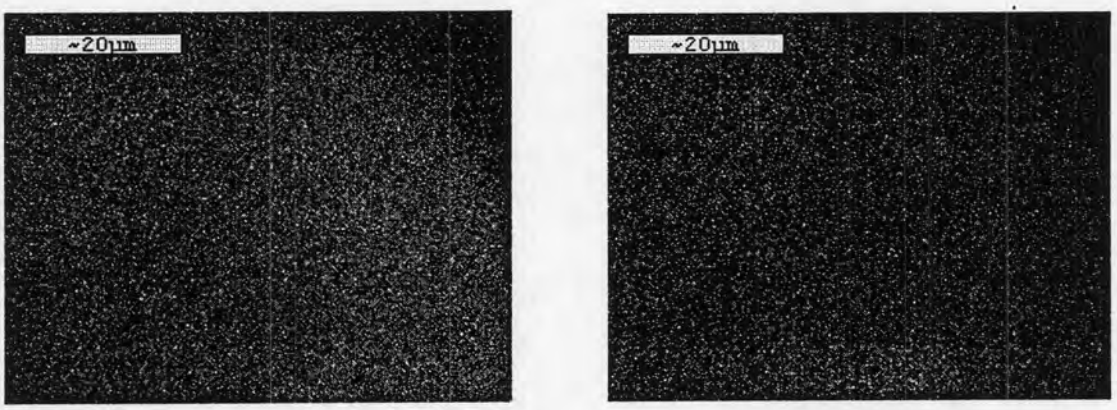


(a) (b)

**Figure 4.7** The EDX of (a) carbon element and (b) aluminium element in AHAMAA prepared with $4x10^{-3}$ mol AA, $2.3x10^{-4}$ mol N-MBA, $1.6x10^{-4}$ mol APS and $12x10^{-4}$ mol TEMED

## 4.2 Determination of residual acrylamide monomer

The residual acrylamide monomer of the poly[AM-*co*-(AA)] with various concentrations of acrylic acid with the fixed N-MBA, APS and TEMED

concentrations at $4.6x10^{-4}$, $3.1x10^{-4}$ and $12x10^{-4}$ mol, respectively, is shown in Table 4.4.

**Table 4.4** Effect of the acrylamide concentration on residual acrylamide monomer of the synthesized poly[AM-*co*-(AA)] [1]

| AM concentration (mol) | Initial acrylamide concentration (ppm) | Residual acrylamide (ppm) | Residual acrylamide (%) |
|---|---|---|---|
| 0.090 | 63972 | 42.648 | 0.067 |
| 0.092 | 65394 | 77.051 | 0.118 |
| 0.094 | 66815 | 62.693 | 0.094 |
| 0.096 | 68237 | 67.810 | 0.099 |
| 0.098 | 69658 | 64.256 | 0.092 |
| 0.100 | 71080 | 62.977 | 0.089 |

[1]Polymerization reactions were carried out with $4.6x10^{-4}$ mol N-MBA, $3.2x10^{-4}$ mol APS, $12x10^{-4}$ mol TEMED, 250 rpm, at 45 °C and 1 h polymerization time

The acrylamide monomers induces human carcinogen and may cause heritable genetic damage. Thus, determination of the residual acrylamide concentration was necessary and beneficial. In this experiment, the residual acrylamide monomer was determined which is directly related to the conversion.

As mentioned earlier, the determination of residual acrylamide monomer was carried out from bromination reaction of acrylamide monomer to form 2,3-

dibromopropionamide. The concentration of 2,3-dibromopropionamide was determined by gas chromatography (model GC-7AG, Shimadzu, Kyoto, Japan).

In addition, the N-MBA ($4.6x10^{-4}$ mol) also take part in the bromination reaction simultaneously with the acrylamide, if the latter is also unreacted in the system. Based on the relative reactivity ratio of the three monomers [r (AM) = 0.58, r (AA) = 1.38, and r (N-MBA) = 1.77] [44], we assumed that the N-MBA concentration could be used up earlier due to two double bonds on a molecule of N-MBA.

From Table 4.4, it indicates that the residual acrylamide monomer was in the range of 42.65-67.81 ppm (0.07-0.10%). This result was independent upon the acrylamide concentration. However, this concentration might have potential health problems because the highest level allowed of a contaminant in drinking water is 0.0005 ppm [45]. To solve the problem of unused or unreacted acrylamide and for economical purposes, one has to reformulate the polymerization recipe. Before this copolymer can be used in drinking water purification, a sequential extraction with hot water must be carried out to remove the unreacted acrylamide and the extractable soluble fractions perhaps the homopolymers of acrylamide at most. For our present research, our aim is to use in dye removal in wastewater treatment.

### 4.3 Determination of water absorbency

The polymeric gels can absorb a large amount of suitable solvents without dissolving because of crosslinked network. The crosslinking agent can induce the network formation of polymeric gels. As more solvent is absorbed by the polymer

network, the network expands progressively. During the swelling process, the network chains are forced to attain more elongated, less probable configurations. As a results, like pulling a spring from both ends, a decrease in chain configurational entropy is produced by swelling. Opposing this, an increase in entropy of mixing of a solvent with a polymer accompanies the swelling. In addition, enthalpy of mixing also controls the extent of swelling.

The equilibrium swelling theory developed by Flory and Rehner treats simple polymer networks in the presence of small molecules. The theory considers forces from three sources [11]:

1. The entropy change caused by mixing a polymer and a solvent. The entropy change from this source is positive and favors swelling.

2. The entropy change by reduction in numbers of possible chain conformations on swelling. The entropy change from this source is negative and opposes swelling.

3. The heat of mixing of polymer and solvent, which may be zero, negative, or positive. Usually, it is slightly positive, opposing mixing.

The major factors contributing to the swelling of ionic networks is ionic content, osmotic pressure, ionization equilibrium, ionic interaction, electrostatic attraction and nature of counterions and so on.

### 4.3.1 Effect of acrylic acid concentration

The water absorbency of the poly[AM-*co*-(AA)] and AHAMAA synthesized by the crosslinking polymerization with various concentrations of acrylic acid and

fixed the N-MBA, APS and TEMED concentrations at $4.6x10^{-4}$, $3.1x10^{-4}$ and $12x10^{-4}$ mol, respectively, is shown in Table 4.5 and Figure 4.8.

**Table 4.5** Effect of acrylic acid concentration on water absorbency ($Q$) of the synthesized poly[AM-*co*-(AA)] [1] and AHAMAA [2]

| Acrylic acid concentration | Water absorbency ($g\ g^{-1}$) | |
|---|---|---|
| ($x\ 10^{-3}$) mol | poly[AM-*co*-(AA)] | AHAMAA |
| 0 | 35±1 | 40±5 |
| 2 | 150±19 | 114±8 |
| 4 | 144±4 | 145±6 |
| 6 | 155±18 | 110±5 |
| 8 | 164±14 | 111±8 |
| 10 | 176±4 | 92±5 |

[1]Polymerization reaction was carried out with $4.6x10^{-4}$ mol N-MBA, $3.2x10^{-4}$ mol APS, $12x10^{-4}$ mol TEMED, 250 rpm, at 45°C and 1 h polymerization time

[2]Polymerization reaction was carried out with $4.6x10^{-4}$ mol N-MBA, $3.2x10^{-4}$ mol APS, $12x10^{-4}$ mol TEMED, 42.5 ml $Al(OH)_3$, 250 rpm, at 45°C and 1 h polymerization time

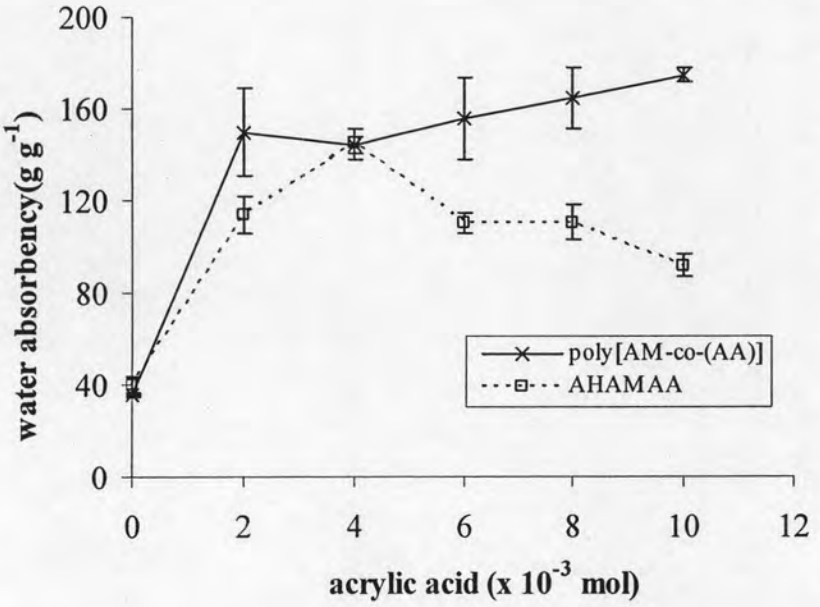


**Figure 4.8** Effect of the acrylic acid concentration on the water absorbency ($Q$) of the poly[AM-*co*-(AA)] and AHAMAA synthesized with $4.6x10^{-4}$ mol N-MBA, $3.2x10^{-4}$ mol APS, $12x10^{-4}$ mol TEMED, 250 rpm, at 45°C and 1 h polymerization time

The water absorbency of poly[AM-*co*-(AA)] and AHAMAA with various acrylic acid concentrations from 0 to $10x10^{-3}$ mol is shown in Figure 4.8. It is indicated that the water absorbency values of poly[AM-*co*-(AA)]s was higher than those of AHAMAAs. The water absorbency of poly[AM-*co*-(AA)] increased with increasing the acrylic acid concentration because increase in the ionic content in polymer network increases the hydrophilicity [11]. The higher hydrophilicity supports the anionic repulsion of carboxylate groups in the polymer chains [13]. The higher the repulsion between those in the polymer chains, the higher the water absorbency can occur [42]. In the case of AHAMAA, the increase in the acrylic acid concentration from 0 to $4x10^{-3}$ mol resulted in a high value of water absorbency as well. The highest water absorbency of AHAMAA of $145\pm6$ g $g^{-1}$ was achieved when the acrylic acid

concentration was $4x10^{-3}$ mol. However, when the acrylic acid content was more than $4x10^{-3}$ mol, the water absorbency decreased. This is resulted from the interaction between the carboxylate anion and counterion, i.e. aluminium ion, by a complex formation to construct the chain rigidity. The complex formation of aluminium ion and the carboxylate anion behaves like another type of crosslinking reaction as shown in Scheme 1, thus it reduced the anionic repulsion [14, 46].

### 4.3.2 Effect of N-MBA concentration

The water absorbency of the poly[AM-*co*-(AA)] and AHAMAA, synthesized with $4x10^{-3}$ mol acrylic acid, $3.2x10^{-4}$ mol APS, $12x10^{-4}$ mol TEMED with various concentrations of the crosslinking agent is shown in Table 4.6 and Figure 4.9.

**Table 4.6** Effect of the crosslinking agent concentration on the water absorbency ($Q$) of the synthesized poly[AM-*co*-(AA)] [1] and AHAMAA [2]

| N-MBA concentration | Water absorbency ($g\ g^{-1}$) | |
|---|---|---|
| (x $10^{-4}$) mol | poly[AM-*co*-(AA)] | AHAMAA |
| 1.2 | 322±13 | 148±2 |
| 2.3 | 205±5 | 142±13 |
| 4.6 | 159±16 | 102±4 |
| 9.2 | 85±3 | 75±2 |

[1]Polymerization reaction was carried out with $4x10^{-3}$ mol AA, $3.2x10^{-4}$ mol APS, $12x10^{-4}$ mol TEMED, 250 rpm, at 45 °C and 1 h polymerization time

[2]Polymerization reaction was carried out with $4x10^{-3}$ mol AA, $3.2x10^{-4}$ mol APS, $12x10^{-4}$ mol TEMED, 42.5 ml $Al(OH)_3$, 250 rpm, at 45°C and 1 h polymerization time

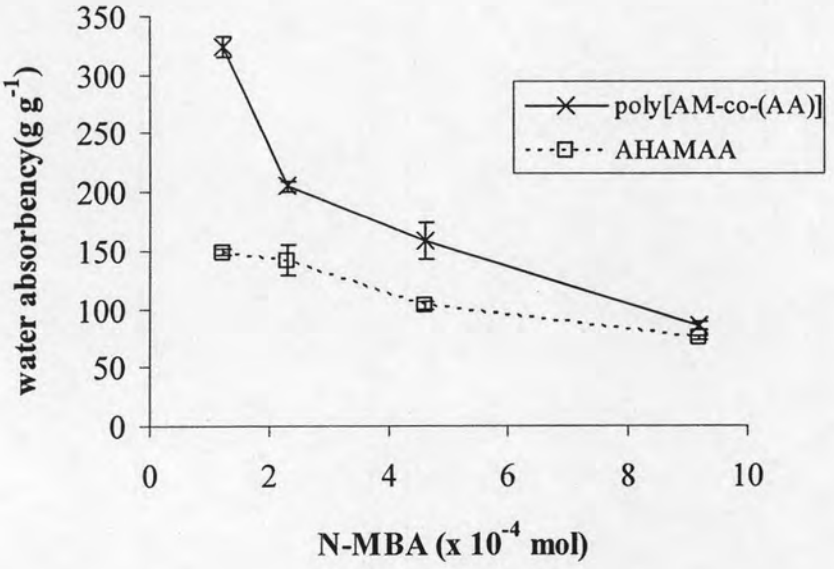


**Figure 4.9** Effect of the crosslinking agent concentration on the water absorbency ($Q$) of the poly[AM-*co*-(AA)] and AHAMAA synthesized with $4x10^{-3}$ mol AA, $3.2x10^{-4}$ mol APS, $12x10^{-4}$ mol TEMED, 250 rpm, at 45 °C and 1 h polymerization time

One factor which can affect the soluble fraction of the poly[AM-*co*-(AA)] and AHAMAA is the relative reactivity ratio of various monomer pairs. In a crosslinking copolymerization, therefore, a bisacrylamide crosslinker will tend to be used up earlier in the reaction to form crosslinking points or junctions.

Basically, the crosslink polymeric gels can be prepared by a chemical reaction to result in a stable chemical binding; on the other hand, it can also be a weak physical link provided by hydrogen bonding between the polar moieties of oxygen or nitrogen atom and the hydrogen atom. Electrostatic attraction between the different polarity of positive and negative charges could also be possible to form a weak physical gel. The

gel was still soft and viscous with sufficient rigidity to hold its integrity and absorb water.

The N-MBA, the crosslinker, has been employed to improve the strength of the swollen gel but the presence of a higher crosslinker concentration can reduce the water absorbency due to an increasing rigid polymer chain [47]. From Figure 4.9, the water absorbency of poly[AM-*co*-(AA)] is of course higher than that of AHAMAA because poly[AM-*co*-(AA)] had only the N-MBA crosslinking. The AHAMAA had both the N-MBA crosslinking and the interaction between aluminium ion and carboxylate anion which reduced the electrostatic repulsion significantly, leading to a decrease in water absorbency [14]. Both poly[AM-*co*-(AA)] and AHAMAA gave the highest water absorbency of $322\pm13$ and $148\pm2$ g $g^{-1}$, respectively, when $1.2\times10^{-4}$ mol of N-MBA was used.

### 4.3.3 Effect of APS concentration

The water absorbency of the crosslinked poly[AM-*co*-(AA)] and AHAMAA, synthesized by $4\times10^{-3}$ mol acrylic acid, $2.3\times10^{-4}$ mol N-MBA, $12\times10^{-4}$ mol TEMED with various initiator (APS) concentrations for the solution polymerization is shown in Table 4.7 and Figure 4.10.

**Table 4.7** Effect of the initiator concentration on water absorbency (*Q*) of the synthesized poly[AM-*co*-(AA)][1] and AHAMAA [2]

| APS concentration | Water absorbency ($g\ g^{-1}$) | |
|---|---|---|
| (x $10^{-4}$) mol | poly[AM-*co*-(AA)] | AHAMAA |
| 0.8 | 211±4 | 144±21 |
| 1.6 | 235±7 | 158±7 |
| 3.1 | 205±5 | 154±6 |
| 6.2 | 166±5 | 115±8 |

[1]Polymerization reaction was carried out with $4x10^{-3}$ mol AA, $2.3x10^{-4}$ mol N-MBA, $12x10^{-4}$ mol TEMED, 250 rpm, at 45 °C and 1 h polymerization time

[2]Polymerization reaction was carried out with $4x10^{-3}$ mol AA, $2.3x10^{-4}$ mol N-MBA, $12x10^{-4}$ mol TEMED, 42.5 ml $Al(OH)_3$, 250 rpm, at 45°C and 1 h polymerization time

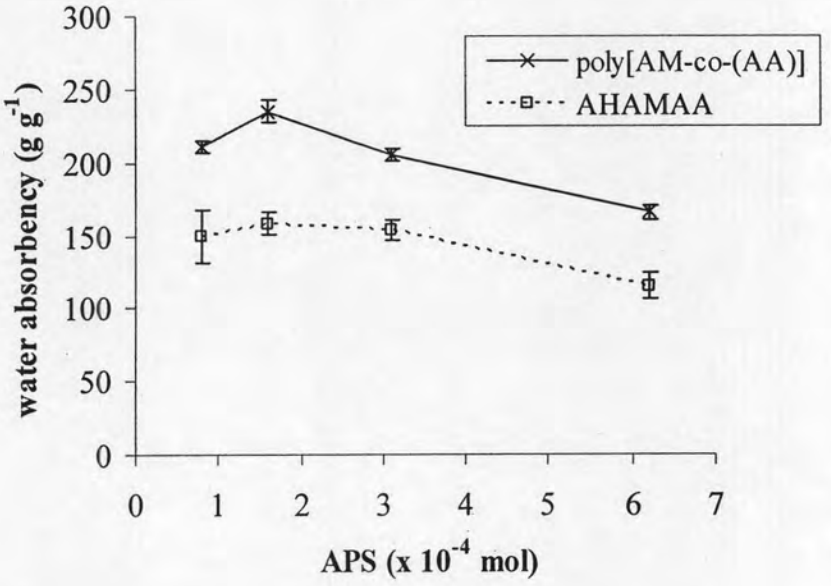


**Figure 4.10** Effect of the initiator concentration on the water absorbency ($Q$) of poly[AM-*co*-(AA)] and AHAMAA synthesized with $4x10^{-3}$ mol AA, $2.3x10^{-4}$ mol N-MBA, $12x10^{-4}$ mol TEMED, 250 rpm, at 45 °C and 1 h polymerization time

In a redox polymerization, a pair of oxidant and reductant is generally used to generate a radical and a pair of cation and anion. Thus, APS and TEMED is another example of oxidation-reduction reactions to produce radicals that can be used to initiate polymerization. The APS, an oxidant, needs to receive an electron from a reductant to start the initiation reaction.

It is well known that the first step in the gel formation process is the initiation reaction between APS, initiator, and TEMED, co-initiator. TEMED is a reducing agent when it reacts with APS. After APS received an electron from TEMED, TEMED molecule was left with an unpaired electron. The activated TEMED

molecule can combine with monomer, which the unpaired electron is transferred to monomer unit, so that it becomes reactive to produce the polymer chains [41, 48].

For a small amount of APS concentration, the water absorbency was low. When the concentration of APS was $1.6x10^{-4}$ mol, the highest water absorbency was achieved. On the other hand, the APS concentration higher than $1.6x10^{-4}$ mol, the water absorbency decreased. At the lower APS concentration, a few radicals were generated and it was insufficient to polymerize until an appropriate chain was realized. At the higher APS concentrations, too many radicals were generated and short polymer chains were resulted in that it cannot swell to a larger extent due to less repulsion attributed by the less amount of the carboxylate group [47]. From Figure 4.10, the water absorbency of AHAMAA was no doubt lower than that of poly[AM-*co*-(AA)] because of complexation between the aluminium ion and the carboxylate anion leading to an reduction of the electrostatic repulsion. However, the highest water absorbency of poly[AM-*co*-(AA)] and AHAMAA was achieved at $235\pm7$ and $158\pm7$ g $g^{-1}$, respectively, when the APS concentration used was $1.6x10^{-4}$ mol.

### 4.3.4 Effect of TEMED concentration

The water absorbency of the crosslinked poly[AM-*co*-(AA)] and AHAMAA, synthesized by $4x10^{-3}$ mol acrylic acid, $2.3x10^{-4}$ mol N-MBA, $1.6x10^{-4}$ mol APS with various co-initiator (TEMED) concentrations for the solution crosslinking polymerization is shown in Table 4.8 and Figure 4.11.

**Table 4.8** Effect of the co-initiator concentration on water absorbency ($Q$) of the synthesized poly[AM-*co*-(AA)] [1] and AHAMAA [2]

| TEMED concentration | Water absorbency ($g\ g^{-1}$) | |
|---|---|---|
| ($x\ 10^{-4}$) mol | poly[AM-*co*-(AA)] | AHAMAA |
| 1.5 | 106±3 | 27±2 |
| 3.0 | 120±3 | 35±4 |
| 6.0 | 215±3 | 60±5 |
| 12.0 | 235±8 | 155±4 |
| 24.0 | 366±31 | 232±18 |
| 36.0 | 538±4 | 294±25 |
| 96.0 | 888±24 | 55±19 |

[1]Polymerization reactions were carried out with $4x10^{-3}$ mol AA, $2.3x10^{-4}$ mol N-MBA, $1.6x10^{-4}$ mol APS, 250 rpm, at 45 °C and 1 h polymerization time

[2]Polymerization reactions were carried out with $4x10^{-3}$ mol AA, $2.3x10^{-4}$ mol N-MBA, $1.6x10^{-4}$ mol APS, 42.5 ml $Al(OH)_3$, 250 rpm, at 45°C and 1 h polymerization time

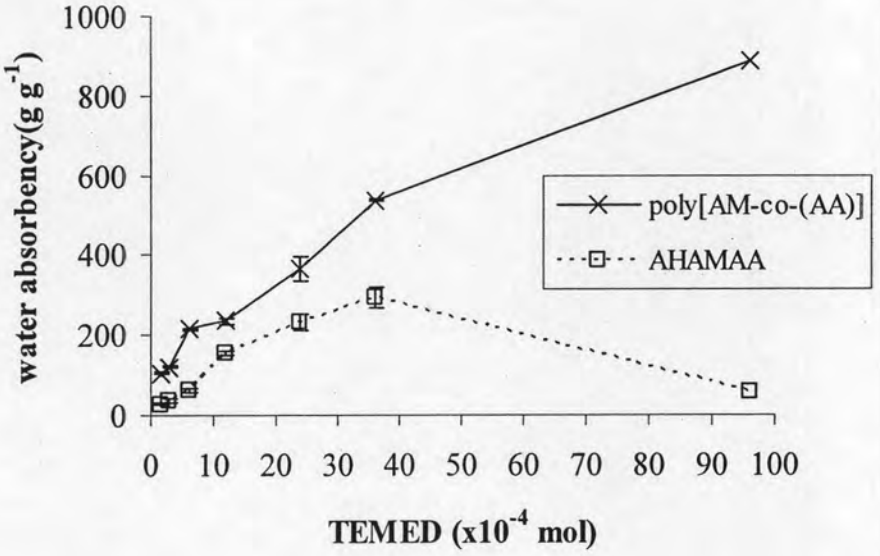


**Figure 4.11** Effect of the co-initiator concentration on the water absorbency ($Q$) of poly[AM-*co*-(AA)] and AHAMAA synthesized with $4x10^{-3}$ mol AA, $2.3x10^{-4}$ mol N-MBA, $1.6x10^{-4}$ mol APS, 250 rpm, at 45 °C and 1 h polymerization time

The TEMED (co-initiator) concentration also affected the water absorbency as shown in Figure 4.11. For both poly[AM-*co*-(AA)] and AHAMAA, the water absorbency increased with increasing the co-initiator concentration. The TEMED accelerated the generation of a higher amount of free radicals to produce the polymer chains. In a redox initiated polymerization, such as the APS and TEMED pair, TEMED generally acts as a reducing agent to generate an electron to reduce the APS, oxidizing agent. In other word, TEMED is co-initiator or starter to induce the decomposition of the initiator, APS. When the TEMED concentration was low, the activated TEMED molecule was not enough to produce hydroxyl radicals. Thus, the long polymer chains were not produced, resulting in the low water absorbency. For

poly[AM-*co*-(AA)], the TEMED concentration of $96x10^{-4}$ mol gave the high water absorbency ($888\pm24$ g $g^{-1}$). This was because the high TEMED concentration produced the short polymer chains which recombined to many longer chains. In the case of AHAMAA, the highest water absorbency of $294\pm25$ g $g^{-1}$ was achieved when the TEMED concentration was $36x10^{-4}$ mol. However, the water absorbency decreased when the TEMED concentration was increased to $96x10^{-4}$ mol. We postulated that the carboxylate anion in the long polymer chains can act as a coordination donor to the reaction site of aluminium ion, leading to many more crosslinking sites in the polymer chain. The high the crosslinking, the greater the chain rigidity and the lower the chain expansion and osmotic pressure. This could be one reason attributed to the very low water absorption.

**4.4 Rheological study**

The strain sweep and frequency sweep of the crosslinked poly[AM-*co*-(AA)] and AHAMAA were monitored using Rheometer (ARES Rheometer, USA) at 25 °C with the parallel plate geometry (50 mm diameter, 1 mm gap). The results are shown in Figures 4.12-4.16.

The strain sweeps were monitored in the range of 0.1-100% at a constant frequency (0.1 rad/s) for determining the linear viscoelastic range, where the storage modulus (G') and loss modulus (G") are independent of the strain amplitude. The strain sweep in Figure 4.12 shows that the linear viscoelastic range is 0.1-10 % strain.

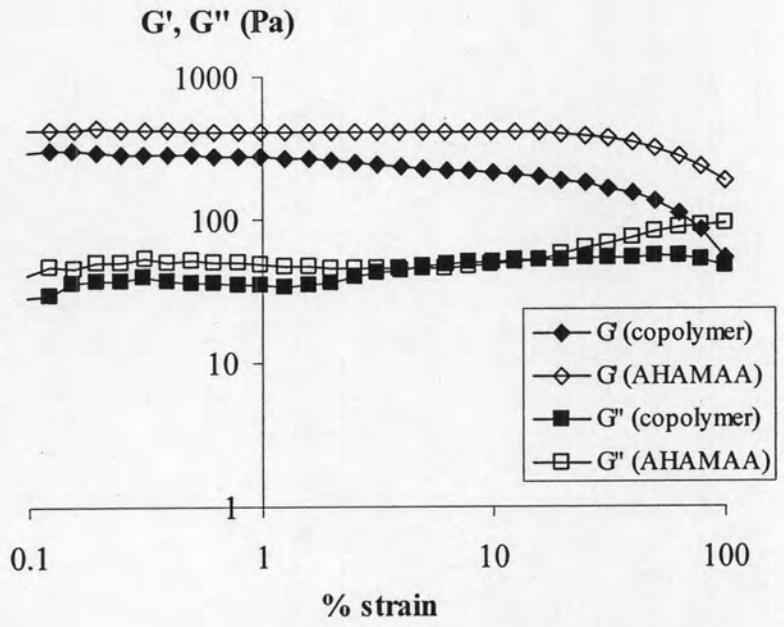


**Figure 4.12** The strain sweep of poly[AM-*co*-(AA)] and AHAMAA at the constant frequency (0.1 rad $s^{-1}$)

Moreover, G' values of poly[AM-*co*-(AA)] and AHAMAA were higher than the G" values. This indicates that the elastic response of the gel was stronger than the viscous response [49]. After the strain sweep, the strain value at 1% was chosen to study the frequency sweeps.

Figure 4.13 represents the importance of the carboxylate anion in acrylic acid and aluminium ion in AHAMAA since G' of AHAMAA with acrylic acid was higher than that of AHAMAA without the acrylic acid content i.e., only PAM superabsorbent polymer Furthermore, the presence of the crosslinking agent and aluminium hydroxide influences the G' values as to be presented in Figures 4.14-4.15.

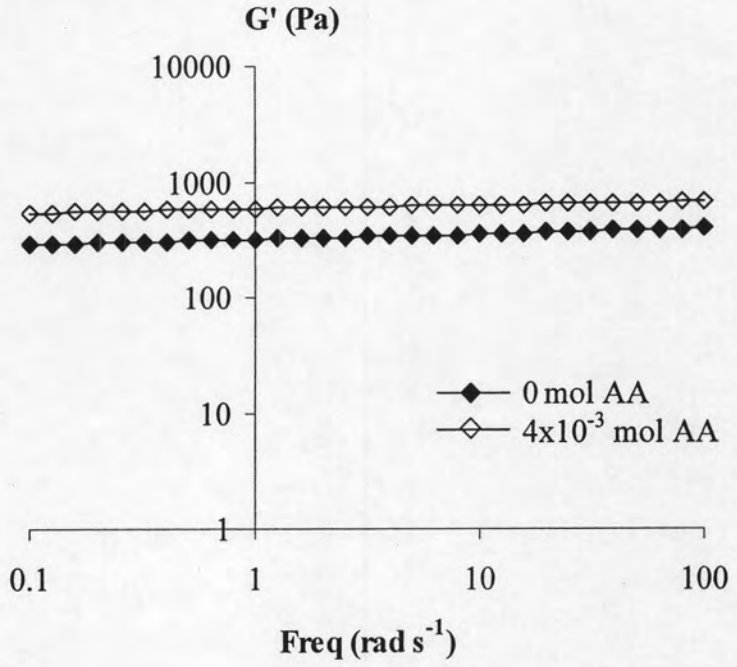


**Figure 4.13** Effect of the acrylic acid of AHAMAA on storage modulus at the constant strain (1% strain)

Figures 4.14 and 4.15 demonstrate that the elastic response of poly[AM-*co*-(AA)] and AHAMAA increased with increasing crosslinking agent concentration because the higher crosslinking agent concentration brings more main chains and joins them together with one or more molecules of the crosslinking agent to become a part of the rigid polymer chains [47]. During the swelling process, the network chains are forced to loosen the chain entanglements and to become more elongated in a similar manner of pulling both ends of a spring.

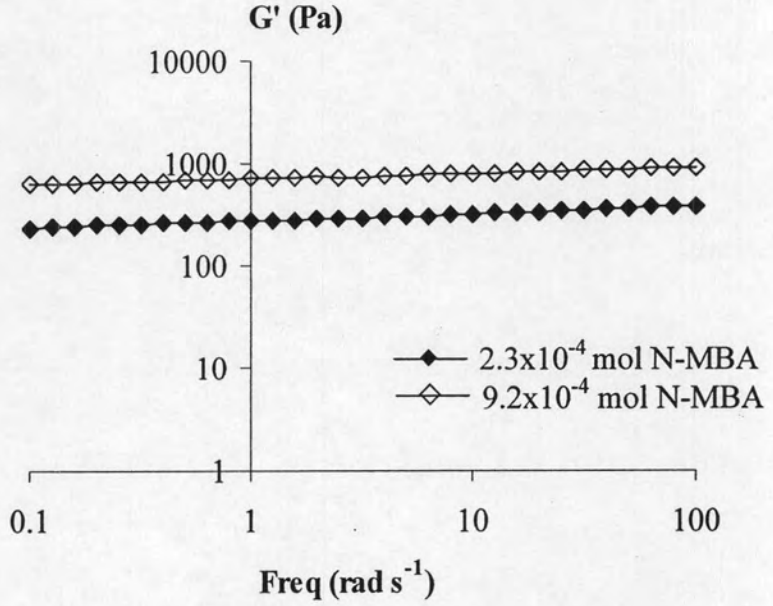


**Figure 4.14** Effect of the crosslinking agent concentration of poly[AM-*co*-(AA)] on storage modulus at a constant strain (1% strain)

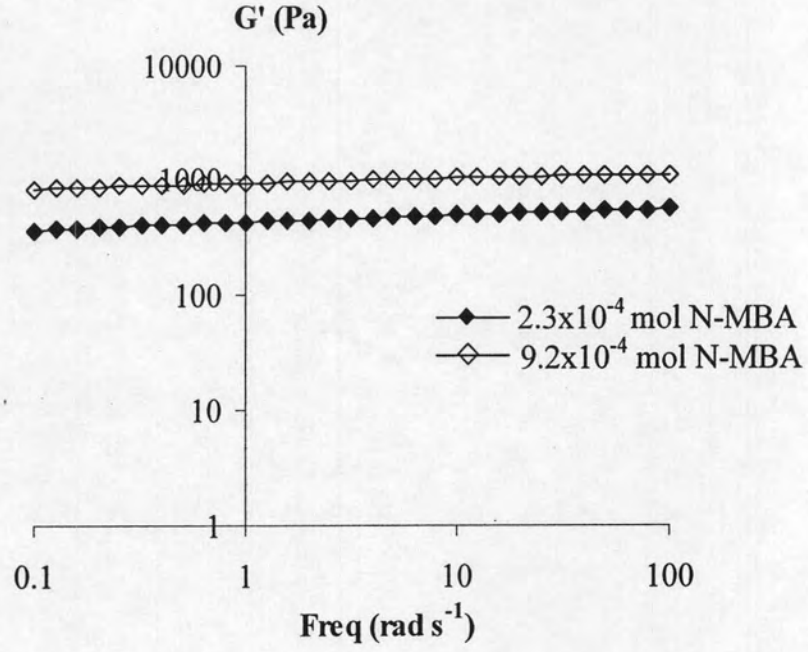


**Figure 4.15** Effect of the crosslinking agent concentration of AHAMAA on storage modulus at a constant strain (1% strain)

At the constant crosslinking agent concentration ($2.3x10^{-4}$ mol), the G' value of poly[AM-*co*-(AA)] was lower than that of AHAMAA as shown in Figure 4.16. Because the chelating interaction between the carboxylate anion and the aluminium ion in AHAMAA induces the chain rigidity, which results in the higher storage modulus. This result can be inversely related to the water absorbency. From Section 4.3.2, both poly[AM-*co*-(AA)] and AHAMAA synthesized with $9.2x10^{-4}$ mol N-MBA had lower water absorbency than that of synthesized with $2.3x10^{-4}$ mol N-MBA. It confirms that the low water absorbency is resulted from the rigid polymer chains.

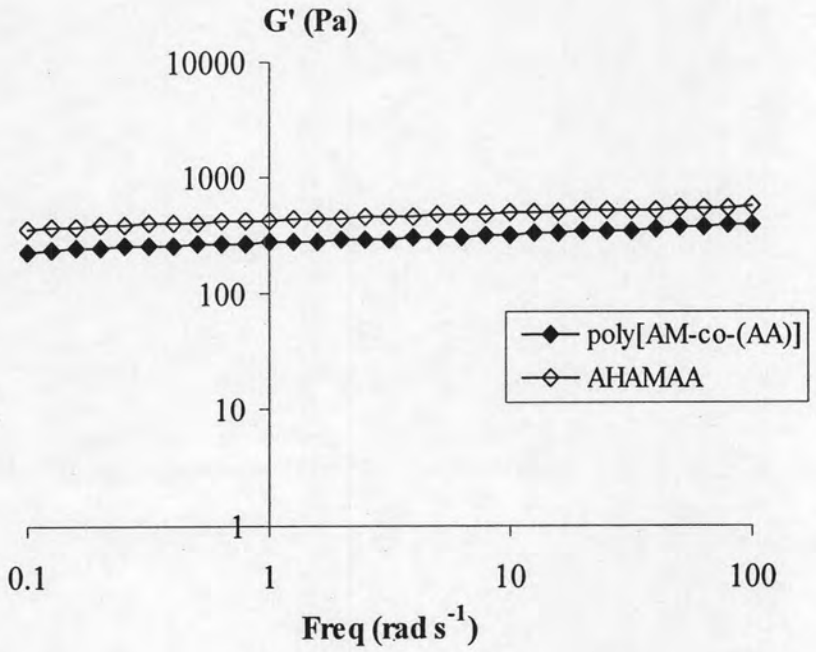


**Figure 4.16** The storage modulus of poly[AM-*co*-(AA)] and AHAMAA at $2.3x10^{-4}$ mol N-MBA at a constant strain (1% strain)

## 4.5 Determination of residual aluminium concentration in the superabsorbent polymer

The aluminium concentration and residual aluminium concentration of the AHAMAA synthesized under the specified conditions are shown in Table 4.9.

**Table 4.9** Aluminium concentration in AHAMAA and residual aluminium in the treating water

| Sample condition | Al in AHAMAA (ppm.) | Residual aluminium (ppm.) retained in the treating water for (days) | | | |
|---|---|---|---|---|---|
| | | 15 | 30 | 45 | 60 |
| A[a] | 9.99±0.51 | 0.15±0.03 | 0.10±0.01 | 0.13±0.03 | 0.17±0.03 |
| B[b] | 11.28±0.78 | 0.19±0.01 | 0.14±0.02 | 0.18±0.02 | 0.14±0.02 |
| C[c] | 13.51±0.38 | 0.16±0.03 | 0.10±0.01 | 0.15±0.01 | 0.13±0.02 |
| D[d] | 10.38±0.55 | 0.15±0.03 | 0.11±0.01 | 0.16±0.02 | 0.14±0.01 |

[a] AA $4x10^{-3}$ mol, N-MBA $4.6x10^{-4}$ mol, APS $3.1x10^{-4}$ mol, TEMED $12x10^{-4}$ mol

[b] AA $4x10^{-3}$ mol, N-MBA $2.3x10^{-4}$ mol, APS $3.1x10^{-4}$ mol, TEMED $12x10^{-4}$ mol

[c] AA $4x10^{-3}$ mol, N-MBA $2.3x10^{-4}$ mol, APS $1.6x10^{-4}$ mol, TEMED $12x10^{-4}$ mol

[d] AA $4x10^{-3}$ mol, N-MBA $2.3x10^{-4}$ mol, APS $1.6x10^{-4}$ mol, TEMED $12x10^{-4}$ mol

The free aluminium ions retained in water lead to Alzheimer's disease when it is intaken in human body. They exhibits strong carcinogenic properties and they have been demonstrated to be toxic especially in the renal function [8]. Therefore, the

determination of the residual aluminium concentration is necessary. The results in Table 4.9 show that the residual aluminium concentration in water was in the range of 0.09-0.2 ppm regardless of the soaking time. It indicates that the stability of aluminium in the AHAMAA was high. Furthermore, this range of the free aluminium concentration had no effect upon the human health. Since the maximum contaminant level of aluminium ion in human body is 0.2 ppm [50]. Therefore, AHAMAA synthesized with various conditions in this experiment is harmless and safe enough to be used as a polymeric flocculant for wastewater treatment.

**4.6 Determination of dye removal efficiency**

One of the aims of this research is the find applications for the two types of superabsorbent polymer and its composite. Dye contaminant in water is one of the hazardous materials for human life. The azo dyes have been blamed for the cause of cancer precursor due to its decomposed product of benzidine [22]. Congo red is one of the azo dyes which has been a potential hazardous dye in human. Therefore, the effect of reaction parameters on the dye removal efficiency was investigated.

Figures 4.17 and 4.18 demonstrate the molecular structures of Congo red and direct blue 71 both of which are called "direct dye" or "anionic dye". Congo red and direct blue 71 contain some similar functional groups, i.e. amino and sulphonate groups but the molecular structure of Congo red is smaller than that of direct blue 71. Therefore, the natures of functional groups and molecular size could affect the absorption capacity of the absorbents.

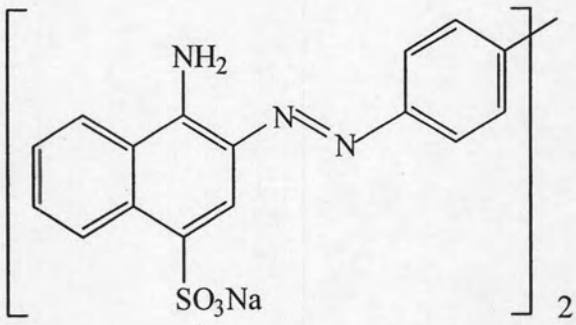


**Figure 4.17** The molecular structure of Congo red (C.I. 21120) [31]

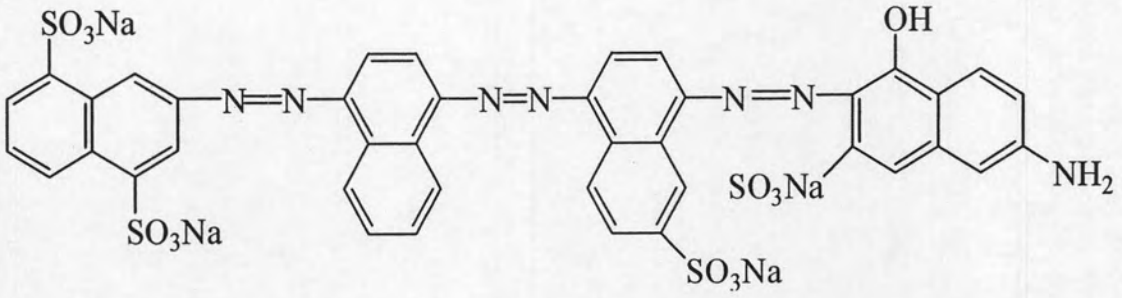


**Figure 4.18** The molecular structure of direct blue 71 (C.I. 34140) [51]

### 4.6.1 Effect of acrylic acid concentration

The Congo red and direct blue 71 removal efficiency of the poly[AM-*co*-(AA)] and AHAMAA synthesized by crosslinking polymerization with various concentrations of acrylic acid and fixed N-MBA, APS and TEMED concentration at $4.6x10^{-4}$, $3.2x10^{-4}$ and $12x10^{-4}$ mol, respectively, is shown in Table 4.10 and Figure 4.19.

**Table 4.10** Effect of the acrylic acid concentration on the dye removal efficiency of the synthesized poly[AM-*co*-(AA)] [1] and AHAMAA [2]

| AA concentration ($x\ 10^{-3}$) mol | %dye removal | | | |
|---|---|---|---|---|
| | Congo red | | Direct blue 71 | |
| | copolymer | AHAMAA | copolymer | AHAMAA |
| 0 | 14±3 | 30±5 | 15±3 | 42±11 |
| 2 | 84±6 | 54±11 | NA[3] | 45±10 |
| 4 | 89±1 | 76±10 | NA[3] | 44±6 |
| 6 | 90±1 | 70±12 | NA[3] | 51±4 |
| 8 | 86±5 | 69±7 | NA[3] | 62±19 |
| 10 | 90±1 | 76±13 | NA[3] | 47±7 |

[1]Polymerization reactions were carried out with $4.6x10^{-4}$ mol N-MBA, $3.2x10^{-4}$ mol APS, $12x10^{-4}$ mol TEMED, 250 rpm, at 45 °C and 1 h polymerization time

[2]Polymerization reactions were carried out with $4.6x10^{-4}$ mol N-MBA, $3.2x10^{-4}$ mol APS, $12x10^{-4}$ mol TEMED, 42.5 ml $Al(OH)_3$, 250 rpm, at 45°C and 1 h polymerization time

[3]Not Available

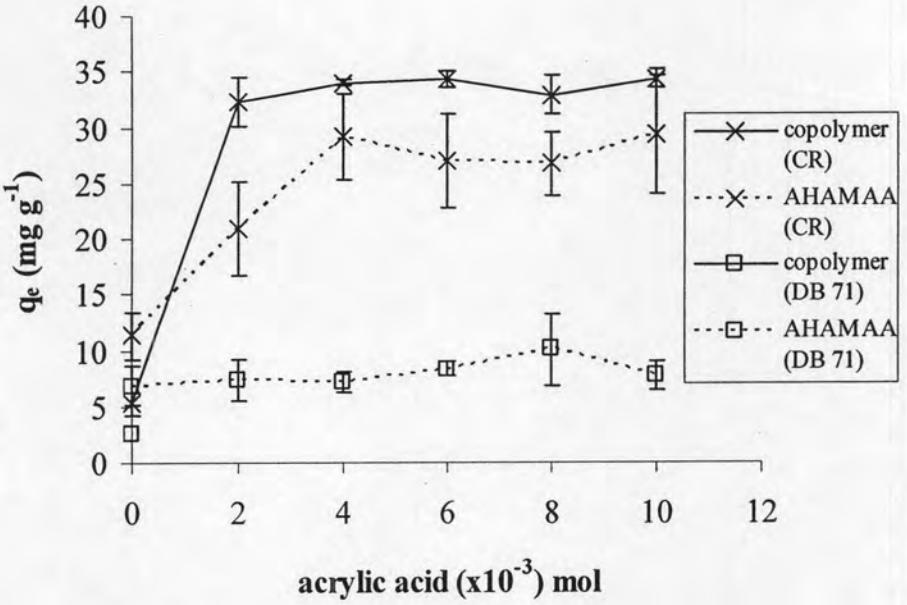


**Figure 4.19** Effect of the acrylic acid concentration on the dye adsorption efficiency of the poly[AM-*co*-(AA)] and AHAMAA synthesized with $4.6x10^{-4}$ mol N-MBA, $3.2x10^{-4}$ mol APS, $12x10^{-4}$ mol TEMED, 250 rpm, at 45°C and 1 h polymerization time

From the results, it indicates that dye removal efficiency of poly[AM-*co*-(AA)]s was higher than that of AHAMAA. For poly[AM-*co*-(AA)], acrylic acid concentration of $2x10^{-3}$ mol was the minimum concentration which could give the best dye removal efficiency. However, this result disagreed with the previous work of Solpan et al. [5], in which poly[AM-*co*-(AA)] could not remove Congo red at all.

In the case of AHAMAA, when the acrylic acid concentration was $4x10^{-3}$ mol, the best dye removal efficiency was achieved because of the interaction between the aluminium ion of AHAMAA and the sulphonate anion of Congo red [38].

The effect of acrylic acid concentration on direct blue 71 removal shows that only AHAMAA could remove direct blue 71, whereas poly[AM-*co*-(AA)] could not. In the case of AHAMAA, the result of the interaction between the aluminium ion of AHAMAA and the sulphonate anion of direct blue 71 was similar to the case of Congo red. However, direct blue 71 had more sulphonate groups which caused the higher repulsion force between the sulphonate group and the carboxylate group of AHAMAA. Thus, the efficiency of AHAMAA for direct blue 71 removal was lower than that of Congo red removal. When the acrylic acid concentration was $8x10^{-3}$ mol, the best direct blue 71 removal efficiency was obtained. The ability of dye removal also depends on water absorption because the dye molecule was uptaken with the absorbing water.

In the case of poly[AM-*co*-(AA)], since it had only the higher repulsion between sulphonate groups of direct blue 71 and the carboxylate groups of poly[AM-*co*-(AA)]. Therefore, it was not effective for the direct blue 71 removal.

Figures 4.20 and 4.21 demonstrate the color and size of poly[AM-*co*-(AA)] and AHAMAA gels after Congo red adsorption and direct blue 71 adsorption, respectively. From Figures 4.20 and 4.21, after the dye adsorption, the gel size of poly[AM-*co*-(AA)] (Figure 4.20 a) was larger than that of AHAMAA (Figure 4.20 b). The weight of swollen poly[AM-*co*-(AA)] and AHAMAA gel after the Congo red adsorption was 159±13 and 109±38 times its dried weight, respectively. In the case of direct blue 71, poly[AM-*co*-(AA)] and AHAMAA gel could swell up to 160±16 and 145±21 times its dried weight, respectively. The higher weight of swollen poly[AM-*co*-(AA)] after the dye adsorption was resulted from the higher water absorbency that had been explained earlier in Section 4.3.4. This result indicates that the dye molecule

also was uptaken with the absorbing water. After the Congo red and direct blue 71 adsorption, the AHAMAA gel had a deeper color than that of poly[AM-*co*-(AA)] because the dye molecules were absorbed into AHAMAA gel which absorption obeys the Freundlich isotherm to be explained in Section 4.7.

The dye removal of AHAMAA synthesized with $4x10^{-3}$ mol of acrylic acid was selected to investigate the effect of N-MBA concentration on dye removal, because this condition gave the best dye removal efficiency.

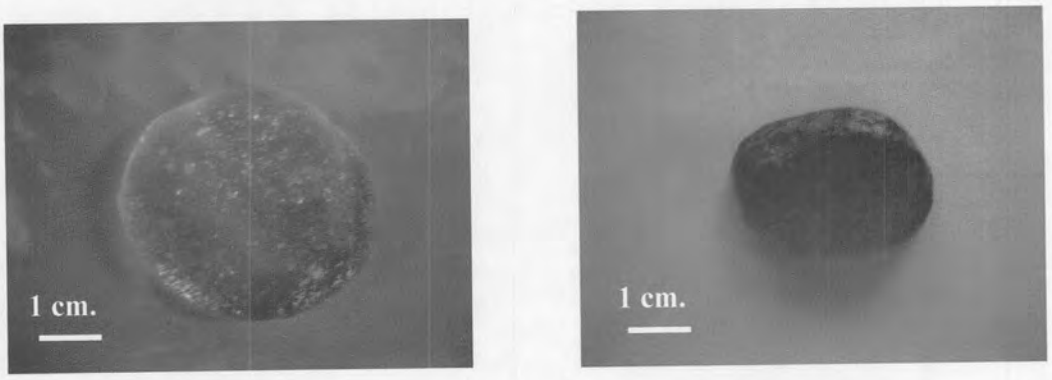


(a) (b)

**Figure 4.20** The swollen gel after Congo red adsorption by (a) poly[AM-*co*-(AA)] and (b) AHAMAA

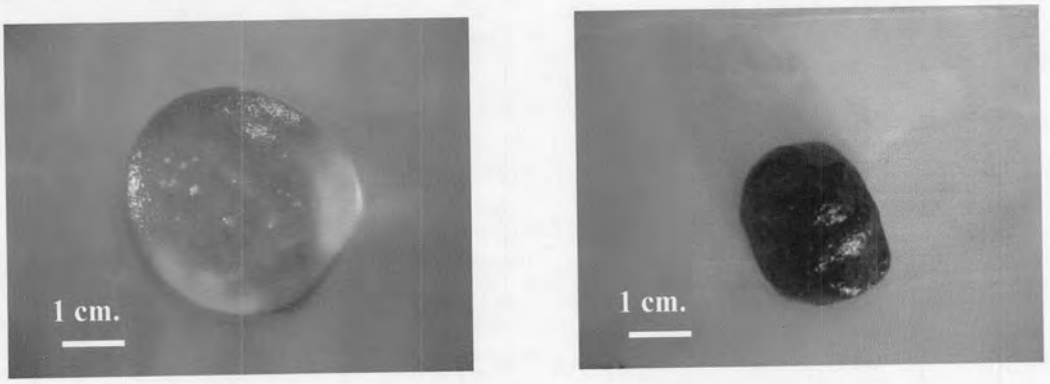


(a) (b)

**Figure 4.21** The swollen gel after direct blue 71 adsorption by (a) poly[AM-*co*-(AA)] and (b) AHAMAA

### 4.6.2 Effect of N-MBA concentration

The dye adsorption ability of the poly[AM-*co*-(AA)] and AHAMAA, synthesized by $4x10^{-3}$ mol of acrylic acid with $3.2x10^{-4}$ mol APS, $12x10^{-4}$ mol TEMED at various concentrations of the N-MBA crosslinking agent is shown in Table 4.11 and Figure 4.22.

**Table 4.11** Effect of the crosslinking agent concentration on the dye removal efficiency of the synthesized poly[AM-*co*-(AA)] [1] and AHAMAA [2]

| N-MBA concentration ($x 10^{-4}$) mol | %dye removal | | | |
|---|---|---|---|---|
| | Congo red | | Direct blue 71 | |
| | copolymer | AHAMAA | copolymer | AHAMAA |
| 1.2 | 88±3 | 82±7 | NA[3] | 63±5 |
| 2.3 | 92±1 | 84±8 | NA[3] | 63±16 |
| 4.6 | 91±1 | 75±11 | NA[3] | 64±13 |
| 9.2 | 91±1 | 81±8 | NA[3] | 71±9 |

[1]Polymerization reactions were carried out with $4x10^{-3}$ mol AA, $3.2x10^{-4}$ mol APS, $12x10^{-4}$ mol TEMED, 250 rpm, at 45 °C and 1 h polymerization time

[2]Polymerization reactions were carried out with $4x10^{-3}$ mol AA, $3.2x10^{-4}$ mol APS, $12x10^{-4}$ mol TEMED, 42.5 ml $Al(OH)_3$, 250 rpm, at 45°C and 1 h polymerization time

[3]Not Available

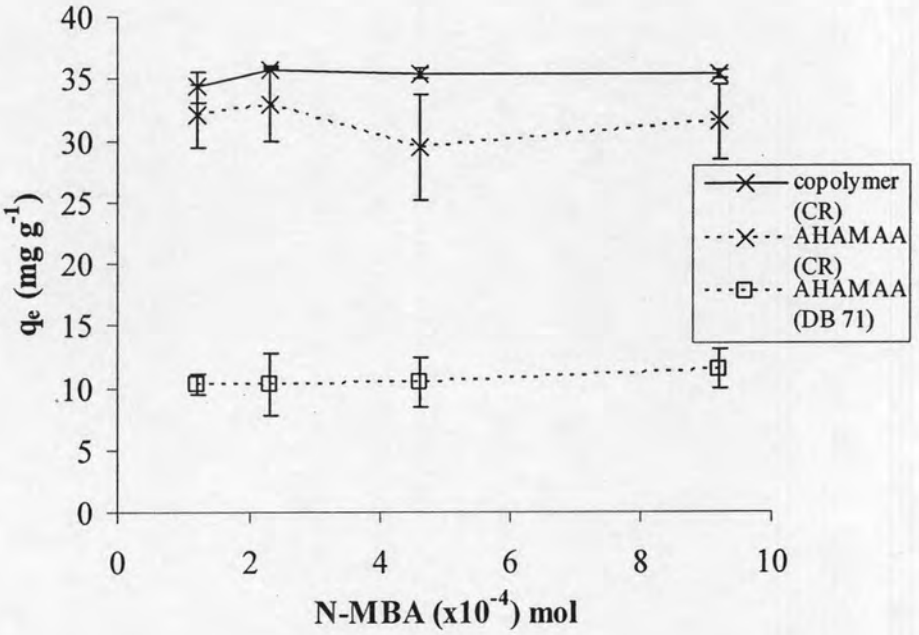


**Figure 4.22** Effect of the crosslinking agent concentration on the dye adsorption efficiency of the poly[AM-*co*-(AA)] and AHAMAA synthesized with $4x10^{-3}$ mol AA, $3.2x10^{-4}$ mol APS, $12x10^{-4}$ mol TEMED, 250 rpm, at 45 °C and 1 h polymerization time

Effect of the crosslinking agent concentration on Congo red and direct blue 71 removal is shown in Figure 4.22. From Figure 4.22, the results show that the N-MBA concentration did not have any effect on the dye removal. Poly[AM-*co*-(AA)] could remove Congo red more than 85% (over 33 mg $g^{-1}$) but could not remove direct blue 71 at all. This is anticipated to result from the molecular size and structure of the dyes. From Figures 4.17 and 4.18, the molecular size of Congo red is smaller than that of direct blue 71, thus Congo red was transported into the open pores in poly[AM-*co*-(AA)] structure [7, 12]. In the case of AHAMAA, it can remove both of the dyes

because of the ion-ion interaction between aluminium ion in AHAMAA and sulphonate anion in dye structures [38]. The efficiency of Congo red and direct blue 71 removal by AHAMAA was in the range of 75-92% (25-36 mg $g^{-1}$) and 63-71% (8-13 mg $g^{-1}$), respectively.

From this section, the AHAMAA synthesized by $2.3x10^{-4}$ mol of N-MBA had the best efficiency for the dye removal. Thus, this condition was selected to further study the effect of initiator on the dye removal.

### 4.6.3 Effect of APS concentration

The dye removal efficiency of the crosslinked poly[AM-*co*-(AA)] and AHAMAA synthesized by $4x10^{-3}$ mol acrylic acid, $2.3x10^{-4}$ mol N-MBA, $12x10^{-4}$ mol TEMED with various initiator (APS) concentrations for the solution polymerization is shown in Table 4.12 and Figure 4.23.

**Table 4.12** Effect of the initiator concentration on the dye removal efficiency of the synthesized poly[AM-*co*-(AA)][1] and AHAMAA[2]

| APS concentration ($x\ 10^{-4}$) mol | %dye removal | | | |
|---|---|---|---|---|
| | Congo red | | Direct blue 71 | |
| | copolymer | AHAMAA | copolymer | AHAMAA |
| 0.8 | 84±4 | 88±6 | NA[3] | 71±2 |
| 1.6 | 87±3 | 93±1 | NA[3] | 62±2 |
| 3.1 | 80±5 | 91±5 | NA[3] | 57±3 |
| 6.2 | 81±1 | 84±5 | NA[3] | 65±2 |

[1]Polymerization reactions were carried out with $4x10^{-3}$ mol AA, $2.3x10^{-4}$ mol N-MBA, $12x10^{-4}$ mol TEMED, 250 rpm, at 45 °C and 1 h polymerization time

[2]Polymerization reactions were carried out with $4x10^{-3}$ mol AA, $2.3x10^{-4}$ mol N-MBA, $12x10^{-4}$ mol TEMED, 42.5 ml $Al(OH)_3$, 250 rpm, at 45°C and 1 h polymerization time

[3]Not Available

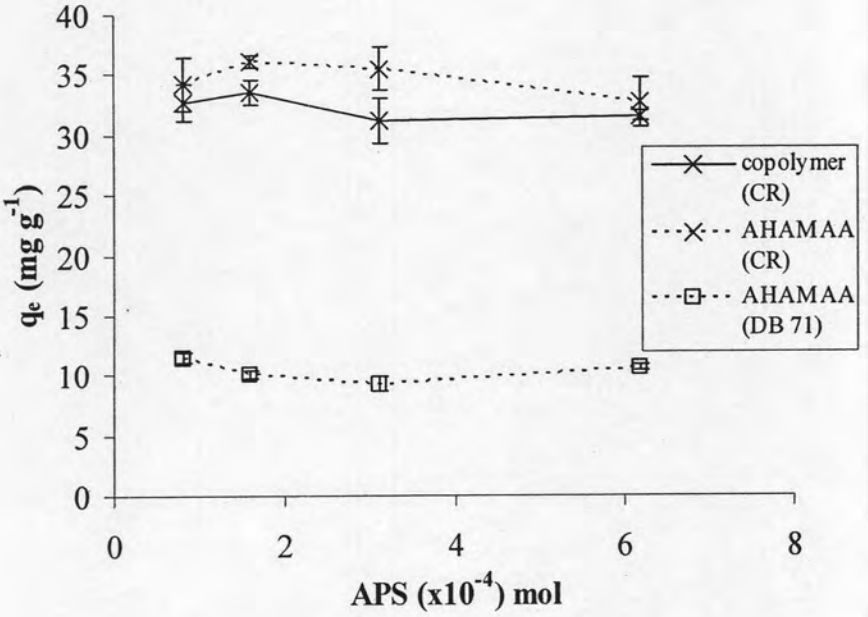


**Figure 4.23** Effect of the initiator concentration on the dye adsorption efficiency of poly[AM-*co*-(AA)] and AHAMAA synthesized with $4x10^{-3}$ mol AA, $2.3x10^{-4}$ mol N-MBA, $12x10^{-4}$ mol TEMED, 250 rpm, at 45 °C and 1 h polymerization time

The efficiency of Congo red and direct blue 71 removal by poly[AM-*co*-(AA)] and AHAMAA is given in Figure 4.23. Considering Congo red removal, the results show that the dye removal efficiency of Congo red by AHAMAA was better than those of poly[AM-*co*-(AA)] synthesized at the same APS concentrations. In the case of direct blue 71, AHAMAA could remove direct blue 71 with all synthesized conditions but poly[AM-*co*-(AA)] could not. This is resulted from the interaction between aluminium ion in AHAMAA and sulphonate anion ($SO_3^-$) in anionic dye structures of direct blue 71 [38].

### 4.6.4 Effect of TEMED concentration

The dye removal efficiency of the crosslinked poly[AM-*co*-(AA)] and AHAMAA, synthesized by $4x10^{-3}$ mol acrylic acid, $2.3x10^{-4}$ mol N-MBA, $1.6x10^{-4}$ mol APS and various co-initiator (TEMED) concentrations for the solution polymerization is shown in Table 4.13 and Figure 4.24.

**Table 4.13** Effect of the co-initiator concentration on the dye removal efficiency of the synthesized poly[AM-*co*-(AA)][1] and AHAMAA [2]

| TEMED concentration ($x10^{-4}$) mol | %dye removal | | | |
|---|---|---|---|---|
| | Congo red | | Direct blue 71 | |
| | copolymer | AHAMAA | copolymer | AHAMAA |
| 1.5 | 13±10 | 63±3 | NA[3] | 89±1 |
| 3 | 89±1 | 64±9 | NA[3] | 87±1 |
| 6 | 90±3 | 86±3 | NA[3] | 88±1 |
| 12 | 89±1 | 91±1 | NA[3] | 66±1 |

[1]Polymerization reactions were carried out with $4x10^{-3}$ mol AA, $2.3x10^{-4}$ mol N-MBA, $1.6x10^{-4}$ mol APS, 250 rpm, at 45 °C and 1 h polymerization time

[2]Polymerization reactions were carried out with $4x10^{-3}$ mol AA, $2.3x10^{-4}$ mol N-MBA, $1.6x10^{-4}$ mol APS, 42.5 ml $Al(OH)_3$, 250 rpm, at 45°C and 1 h polymerization time

[3]Not Available

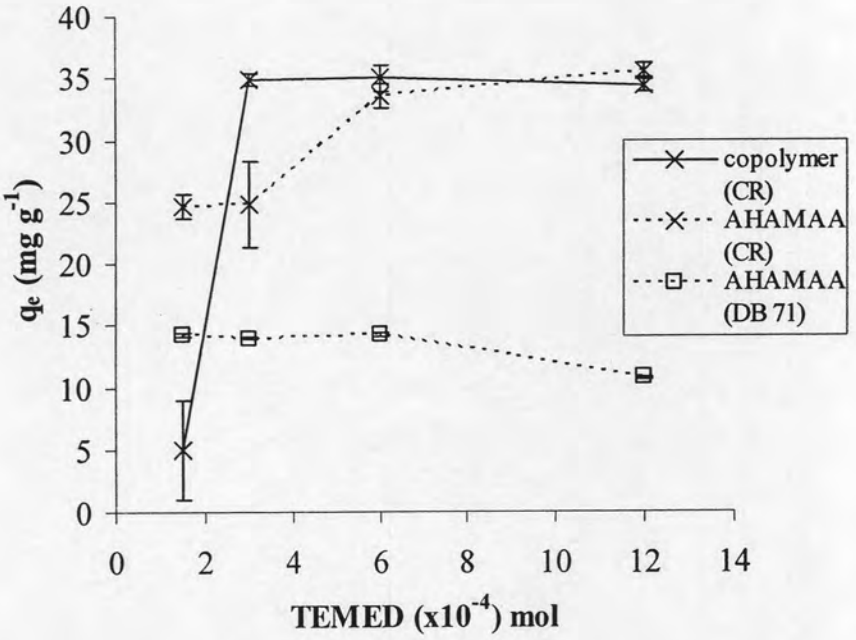


**Figure 4.24** Effect of the co-initiator concentration on the dye removal efficiency of poly[AM-*co*-(AA)] and AHAMAA synthesized with $4x10^{-3}$ mol AA, $2.3x10^{-4}$ mol N-MBA, $1.6x10^{-4}$ mol APS, 250 rpm, at 45 °C and 1 h polymerization time

From $3x10^{-4}$ to $12x10^{-4}$ mol of TEMED, the TEMED concentration had a constant efficiency on Congo red removal by poly[AM-*co*-(AA)] as shown in Figure 4.24. AHAMAA had a better efficiency of Congo red removal than that of poly[AM-*co*-(AA)] and gave the best efficiency at $12x10^{-4}$ mol of TEMED which could remove Congo red of 91% (36 mg $g^{-1}$).

In the case of direct blue 71 removal, AHAMAA could remove direct blue 71, whereas poly[AM-*co*-(AA)] could not. The best efficiency was achieved at a nearly constant range of 86-90% (14 mg $g^{-1}$) when the TEMED concentration was in the range of $1.5x10^{-4}$ to $6x10^{-4}$ mol.

### 4.6.5 Effect of pH on the dye removal

**a) In a non-buffered system**

The effects of pH on the dye removal efficiency of the synthesized poly[AM-*co*-(AA)] and AHAMAA were investigated by the fixed concentrations of acrylic acid, N-MBA, APS and TEMED at $4x10^{-3}$, $2.3x10^{-4}$, $1.6x10^{-4}$ and $12x10^{-4}$ mol, respectively. The result is shown in Table 4.14.

**Table 4.14** Effect of non-buffered pH on the dye removal efficiency of the synthesized poly[AM-*co*-(AA)] [1] and AHAMAA [2]

| pH | % dye removal | | | |
|---|---|---|---|---|
| | Congo red | | Direct blue 71 | |
| | copolymer | AHAMAA | copolymer | AHAMAA |
| 5 | 82±4 | 93±0 | NA[3] | 61±2 |
| 7 | NA | 20±3 | NA[3] | NA[3] |
| 9 | NA[3] | NA[3] | NA[3] | NA[3] |
| 11 | NA[3] | NA[3] | NA[3] | NA[3] |

[1]Polymerization reactions were carried out with $4x10^{-3}$ mol AA, $2.3x10^{-4}$ mol N-MBA, $1.6x10^{-4}$ mol APS, $12x10^{-4}$ mol TEMED, 250 rpm, at 45 °C and 1 h polymerization time

[2]Polymerization reactions were carried out with $4x10^{-3}$ mol AA, $2.3x10^{-4}$ mol N-MBA, $1.6x10^{-4}$ mol APS, $12x10^{-4}$ mol TEMED, 42.5 ml $Al(OH)_3$, 250 rpm, at 45°C and 1 h polymerization time

[3]Not Available

Since the color of Congo red changes from red to dark blue at pH 3-5, resulting from the changing of the dye molecular structure [31], therefore in this Section, the pH of dye solutions was prepared in the range of 5-11 by adjusting the pH with 0.1 M HCl or 0.1 M NaOH. The result is shown in Table 4.14, poly[AM-*co*-(AA)] could remove Congo red when the solution pH was 5 (82±4% dye removal)

which was similar to in the buffered system (83±2% dye removal). Since the pH of buffered system was adjusted with tri-sodium phosphate, citric acid and boric acid, therefore the difference of a non-buffered system and a buffered system is only the anions and the cations in each solution. It indicated that the presence of different ions in the non-buffered and buffer solution did not affect the Congo red removal. Thus, the efficiency of Congo red removal may result from the transportation of Congo red into the open pores in poly[AM-*co*-(AA)] structure as explained in Section 4.6.2. This result was corresponding to Congo red adsorption isotherm which showed neither the Langmuir nor the Freundlich isotherm to be explained in Section 4.7. In the case of pH 7 to 11, poly[AM-*co*-(AA)] could not remove Congo red. This is because the structure of Congo red and poly[AM-*co*-(AA)] have the sulphonate anion and carboxylate anion, respectively. The repulsion force of both anions resulted in no efficiency for Congo red removal.

In the case of direct blue 71, the results shows that poly[AM-*co*-(AA)] could not remove this dye with various non-buffered pHs (5-11) either because of the repulsion between carboxylate anion (basic form of carboxylic acid) in poly[AM-*co*-(AA)] and more sulphonate anions in the molecule of direct blue 71 [5, 24].

For AHAMAA, it could remove Congo red at pH 5 with a high dye removal percentage (93±0%). This was due to the attraction of cationic part (aluminium ion) and the anionic moiety in the dye molecule at this pH. When the solution pH was 7, the salt form of the carboxylic acid groups dominated, leading into the repulsion between the sulphonate anion in dye molecule and negative charge ($COO^-$) in AHAMAA. Thus, the Congo red removal efficiency was decreased from 93±0 to

20±3%. At pH 9-11, AHAMAA could not remove Congo red at all. This was due to the repulsion between the anionic part of both AHAMAA and Congo red. In addition, aluminium ion (cationic part) in AHAMAA might react with hydroxide ion at high pH instead of the anion of dye.

In the case of direct blue 71, the results showed that AHAMAA could remove the dye at pH 5 (61±2% dye removal) which were lower than that of Congo red. This was due to the more sulphonate group, leading into the higher repulsion with the carboxylate anion in AHAMAA. At pH 7-11, AHAMAA could not remove direct blue 71. The reason was explained in the case of Congo red at pH 9-11.

**b) In a buffered system**

The effects of the ionic strength of the pH solution on dye removal efficiency of the crosslinked poly[AM-*co*-(AA)] and AHAMAA was investigated by the fixed concentrations of acrylic acid, N-MBA, APS and TEMED at $4x10^{-3}$, $2.3x10^{-4}$, $1.6x10^{-4}$ and $12x10^{-4}$ mol, respectively. The results are shown in Table 4.15 and Figure 4.25.

**Table 4.15** Effect of the ionic strength on the dye removal efficiency of the synthesized poly[AM-*co*-(AA)] [1] and AHAMAA [2]

| pH | Ionic strength (mol-ion $dm^{-3}$) | % dye removal | | | |
|---|---|---|---|---|---|
| | | Congo red | | direct blue 71 | |
| | | copolymer | AHAMAA | copolymer | AHAMAA |
| 5 | 1.203 | 83±2 | 28±4 | 2±1 | 35±7 |
| 7 | 1.046 | 6±2 | 3±1 | 2±0 | 2±1 |
| 9 | 0.911 | 3±1 | 3±2 | 1±1 | NA[3] |
| 11 | 0.798 | 1±1 | NA[3] | NA[3] | NA[3] |

[1]Polymerization reactions were carried out with $4x10^{-3}$ mol AA, $2.3x10^{-4}$ mol N-MBA, $1.6x10^{-4}$ mol APS, $12x10^{-4}$ mol TEMED, 250 rpm, at 45 °C and 1 h polymerization time

[2]Polymerization reactions were carried out with $4x10^{-3}$ mol AA, $2.3x10^{-4}$ mol N-MBA, $1.6x10^{-4}$ mol APS, $12x10^{-4}$ mol TEMED, 42.5 ml $Al(OH)_3$, 250 rpm, at 45°C and 1 h polymerization time

[3]Not Available

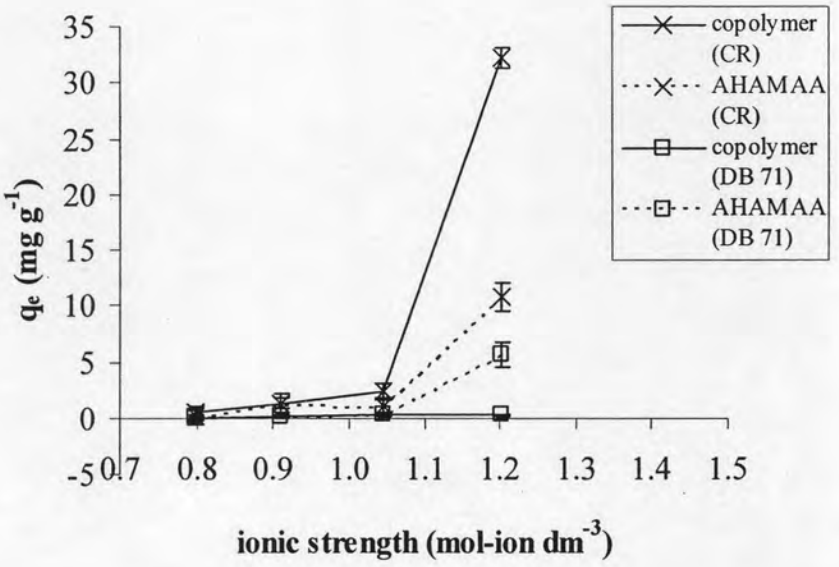


**Figure 4.25** Effect of the ionic strength on the dye removal efficiency of poly[AM-*co*-(AA)] and AHAMAA synthesized with $4x10^{-3}$ mol AA, $2.3x10^{-4}$ mol N-MBA, $1.6x10^{-4}$ mol APS, $12x10^{-4}$ mol TEMED, 250 rpm, at 45 °C and 1 h polymerization time

As mentioned in the section of non-buffered system, the pH of dye solution was prepared in the range of 5-11 by adjusting the pH with the buffer solution of tri-sodium phosphate, citric acid and boric acid. The result is shown in Table 4.15 in which the efficiency of Congo red removal by poly[AM-*co*-(AA)] in the buffered system (82±4%) was similar to those of the non-buffered system (83±2%) at pH 5 (ionic strength 1.203 mol-ion $dm^{-3}$). This was resulted from the transportation of Congo red solution into the open pores in poly[AM-*co*-(AA)] structure as explained in the section of non-buffered system. In the case of direct blue 71, poly[AM-*co*-(AA)] could not remove direct blue 71 because of the higher repulsion of carboxylate anion

in poly[AM-*co*-(AA)] structure and sulphonate anion in the dye structure. In the case of AHAMAA, it could remove both Congo red and direct blue 71 which was similar to the non-buffered system. Very interestingly, the dye removal efficiency in the non-buffered system of AHAMAA was significantly higher than those of the buffered system at pH 5. Because the presence of citrate anion and/or borate anion, which is the low molecular weight organic acid, in the buffer solution creates a complex formation between aluminium ion [52] in AHAMAA and citrate anion and/or borate anion (Figure 4.26 b), leading into a decreasing attraction between aluminium ion and sulphonate anion in the dye structure and a lowering dye removal. Moreover, the repulsion of citrate anion and sulphonate anion may also affect the decreasing of dye removal efficiency.

The ionic strength of the solution is a function of the concentration of all ions that present in a solution as shown in Eq. (3.3) and it is one of the factors that control the interactions between the adsorbate and adsorbent surface. However, the ionic strength effect can be seen clearly when the pH of system is fixed at the same pH in all experiments.

Considering the effect of ionic strength on the dye removal efficiency at pH 5 in the buffered and non-buffered system, it indicated that the ionic strength did not affect the Congo red removal by poly[AM-*co*-(AA)]. This was resulted from the transportation of Congo red into the pores of poly[AM-*co*-(AA)] structure. In the case of AHAMAA, the effect of ionic strength on the dye removal was significant at pH 5. The presence of high concentration of cation and anion in the buffered system of Congo red and direct blue 71 may reduce the electrostatic interaction between AHAMAA and the dye molecule [52].

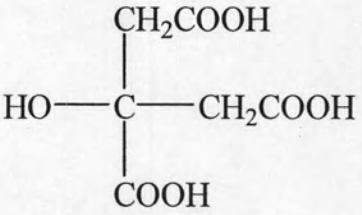


(a)

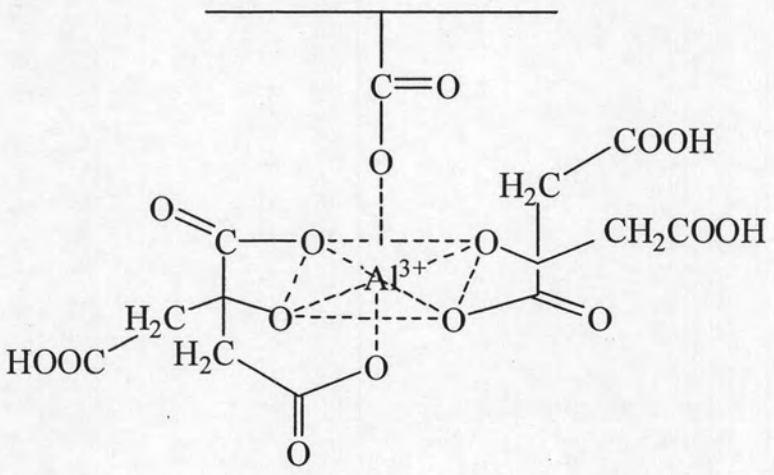


(b)

**Figure 4.26** (a) The molecular structure of citric acid

(b) A possible structure of Al-citrate complex in the buffered system

**4.7 Adsorption isotherm**

The relationship between the amount of a substance adsorbed and its concentration in the equilibrium solution is called adsorption isotherm. The two types of isotherm for describing this experiment are Langmuir isotherm and Freundlich model.

### 4.7.1 The Langmuir isotherm

The Langmuir isotherm represents the model of monolayer adsorption. This isotherm is given as shown in Eq. 2.1 [37]:

$$q_e = \frac{Q_{\max} K_L C_e}{1 + K_L C_e} \tag{2.1}$$

The constants $Q_{max}$ and $K_L$ can be determined from Eq. 2.2 which is a linear form of Eq. 2.1

$$\frac{C_e}{q_e} = \frac{1}{Q_{\max} K_L} + \frac{C_e}{Q_{\max}} \tag{2.2}$$

where $C_e$ is the concentration of dye solution (mg $l^{-1}$) at equilibrium, $q_e$ is the amount of dye adsorbed per unit weight of poly[AM-*co*-(AA)] or AHAMAA (mg $g^{-1}$), $Q_{max}$ is the monolayer capacity of the adsorbent (mg $g^{-1}$) and $K_L$ is the Langmuir adsorption constant (l $mg^{-1}$).

### 4.7.2 The Freundlich isotherm

The Freundlich isotherm reveals the multilayer adsorption model [37]. This model has been presented in Eq. 2.3 [37]:

$$q_e = K_F C_e^{\frac{1}{n}} \tag{2.3}$$

The linear form of Eq. 2.3 can be given as in Eq. 2.4

$$\ln q_e = \ln K_F + \frac{1}{n} \ln C_e \tag{2.4}$$

where $C_e$ is the concentration of dye solution (mg $l^{-1}$) at equilibrium, $K_F$ is the sorption capacity (mg $g^{-1}$) and $n$ is an empirical parameter.

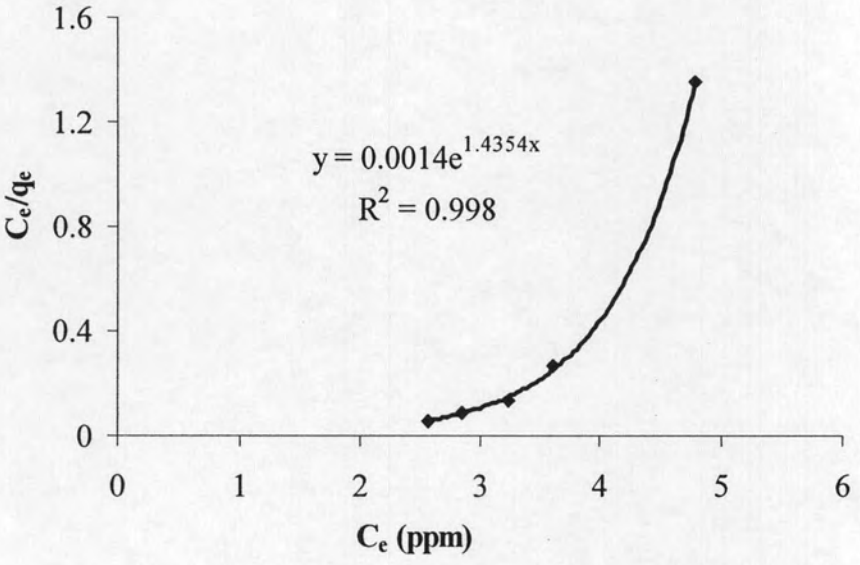


**(a)**

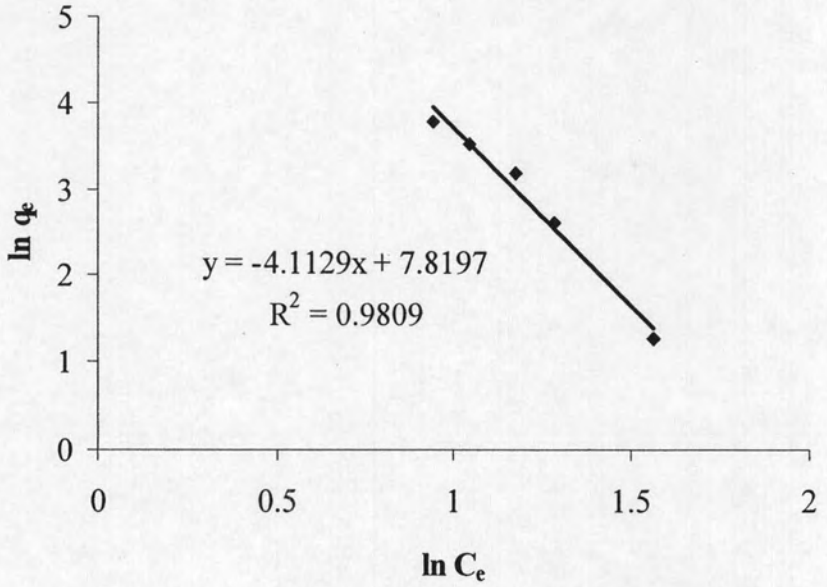


**(b)**

**Figure 4.27** Adsorption isotherm of Congo red by poly[AM-*co*-(AA)]: (a) Langmuir isotherm (b) Freundlich isotherm

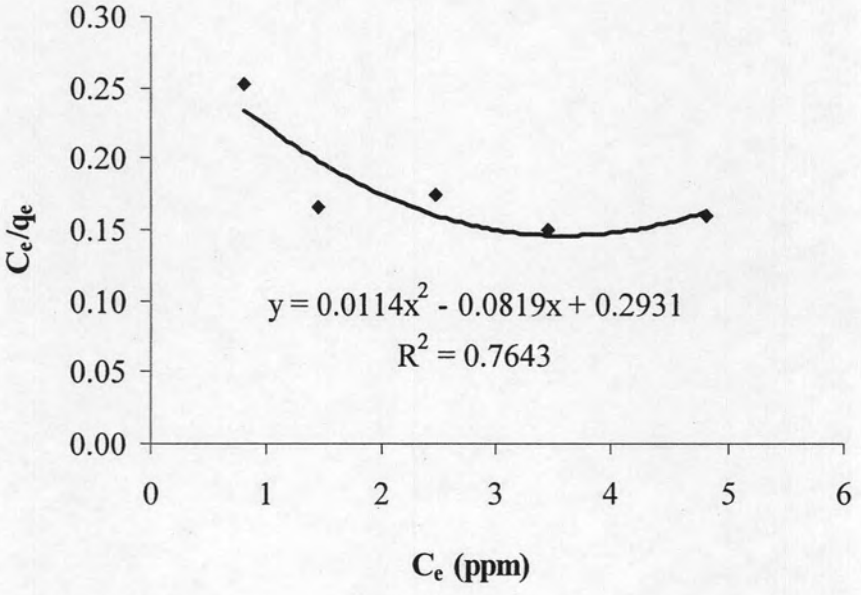


**(a)**

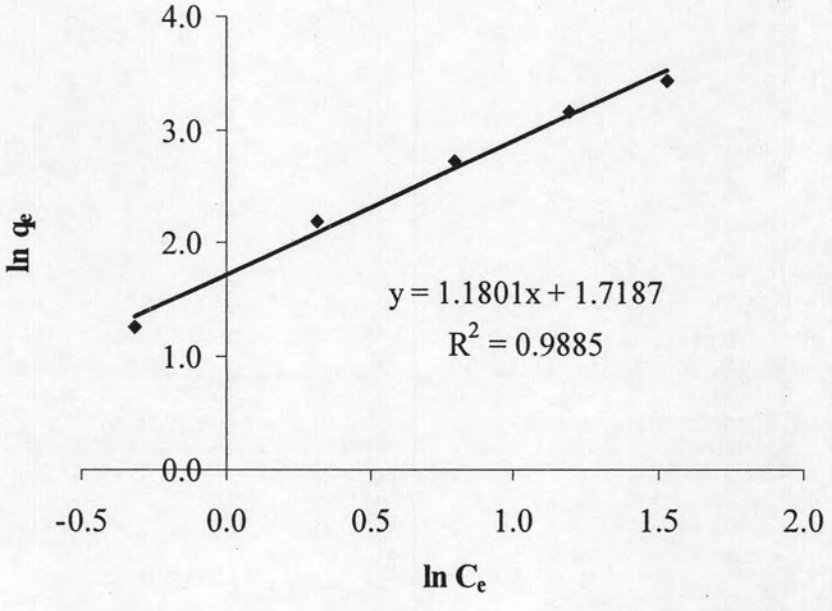


**(b)**

**Figure 4.28** Adsorption isotherm of Congo red by AHAMAA: (a) Langmuir isotherm (b) Freundlich isotherm

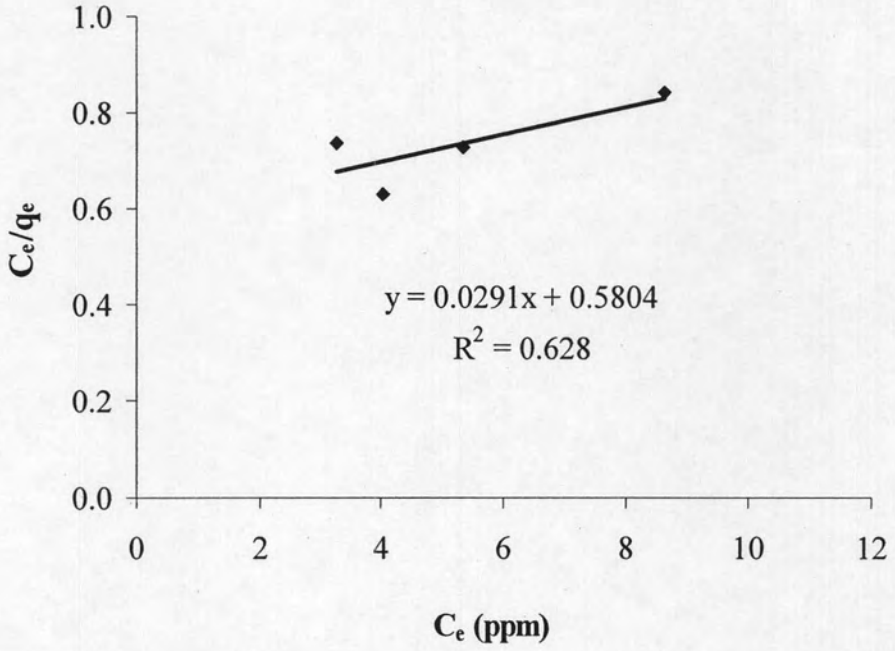


**(a)**

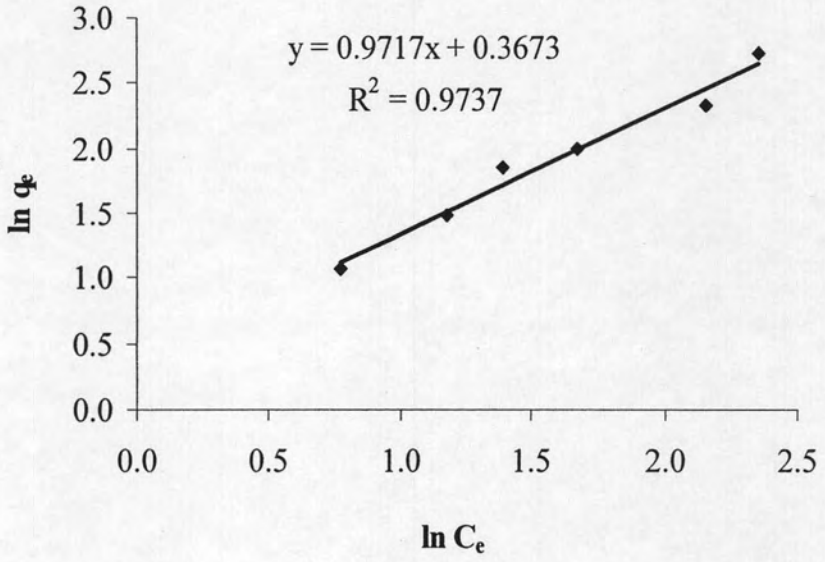


**(b)**

**Figure 4.29** Adsorption isotherm of direct blue 71 by AHAMAA: (a) Langmuir isotherm (b) Freundlich isotherm

Considering the adsorption of Congo red by poly[AM-*co*-(AA)] in Figures 4.27 a and 4.27 b, it did not obey both the Langmuir and Freundlich equations because it did not show the linear relationship in Eqs. 2.2 and 2.4, respectively. The adsorption could occur because the dye solution was transported into the open pores in poly[AM-*co*-(AA)] gel and these pores act as the reservoir for the dye solution storage [7, 12]. In the case of AHAMAA, the adsorption isotherms of Congo red and direct blue 71 did not explain the Langmuir isotherm (Figures 4.28 a and 4.29 a). However, they could obey the Freundlich model evidenced by the linear relationship of $ln\ q_e$ and $ln\ C_e$ with a correlation coefficient ($R^2$) of 0.9885 and 0.9737 as shown in Figure 4.28 b and 4.29 b, respectively. The Freundlich isotherm demonstrates the multilayer adsorption model and describes the adsorption behavior on heterogeneous surfaces [31]. The constants of the Freundlich isotherms, $K_F$ and $n$, obtained from the intercept and slope of the plot in the linear form, respectively, are given in Table 4.16. The $K_F$ is a Freundlich constant that shows the adsorption capacity of the adsorbent. The $n$ is a constant which shows an extent of relationship between adsorbate and adsorbent. The Freundlich isotherm constant, $K_F$, for Congo red and direct blue 71 are 5.58 and 1.44, respectively, and $n$ for Congo red and direct blue are 0.85 and 1.03, respectively. Comparing the relationship of $K_F$, $n$ and $q_e$ values for Congo red and direct blue 71 adsorptions in Table 4.16, $K_F$ and $n$ values of Congo red reflects the higher $q_e$ value, it thus indicates that AHAMAA can adsorb more Congo red than it does on direct blue 71. These results are in good agreement with those previously presented in Section 4.6.4.

**Table 4.16** Freundlich isotherm constants of Congo red and direct blue 71 by AHAMAA adsorption

| Freundlich isotherm constants | values | |
|---|---|---|
| | Congo red | Direct blue 71 |
| $K_F$ | 5.58 | 1.44 |
| $n$ | 0.85 | 1.03 |

### 4.8 Turbidity reduction by the superabsorbent polymers

The effect of flocculation time on the turbidity reduction of the kaolin suspension by the crosslinked poly[AM-*co*-(AA)] and AHAMAA was investigated. The polymers were prepared with the fixed concentrations of acrylic acid, N-MBA, APS and TEMED at $4x10^{-3}$, $2.3x10^{-4}$, $1.6x10^{-4}$ and $12x10^{-4}$ mol, respectively. The results are shown in Table 4.17 and Figures 4.30-4.31.

**Table 4.17** Effect of flocculation time on relative turbidity of the kaolin suspension by the synthesized poly[AM-*co*-(AA)] [1] and AHAMAA[2]

| Flocculation time | Relative turbidity of kaolin | | % Reduction in turbidity | |
|---|---|---|---|---|
| (hours) | copolymer | AHAMAA | copolymer | AHAMAA |
| 0 | 1.00±0.18 | 1.00±0.16 | - | - |
| 3 | 0.18±0.06 | 0.15±0.01 | 82 | 85 |
| 6 | 0.18±0.04 | 0.14±0.02 | 82 | 86 |
| 9 | 0.18±0.04 | 0.12±0.03 | 82 | 88 |
| 15 | 0.17±0.05 | 0.08±0.02 | 83 | 92 |
| 24 | 0.16±0.04 | 0.05±0.01 | 84 | 95 |

[1]Polymerization reaction was carried out with $4x10^{-3}$ mol AA, $2.3x10^{-4}$ mol N-MBA, $1.6x10^{-4}$ mol APS, $12x10^{-4}$ mol TEMED, 250 rpm, at 45 °C and 1 h polymerization time

[2]Polymerization reactions were carried out with $4x10^{-3}$ mol AA, $2.3x10^{-4}$ mol N-MBA, $1.6x10^{-4}$ mol APS, $12x10^{-4}$ mol TEMED, 42.5 ml $Al(OH)_3$, 250 rpm, at 45°C and 1 h polymerization time

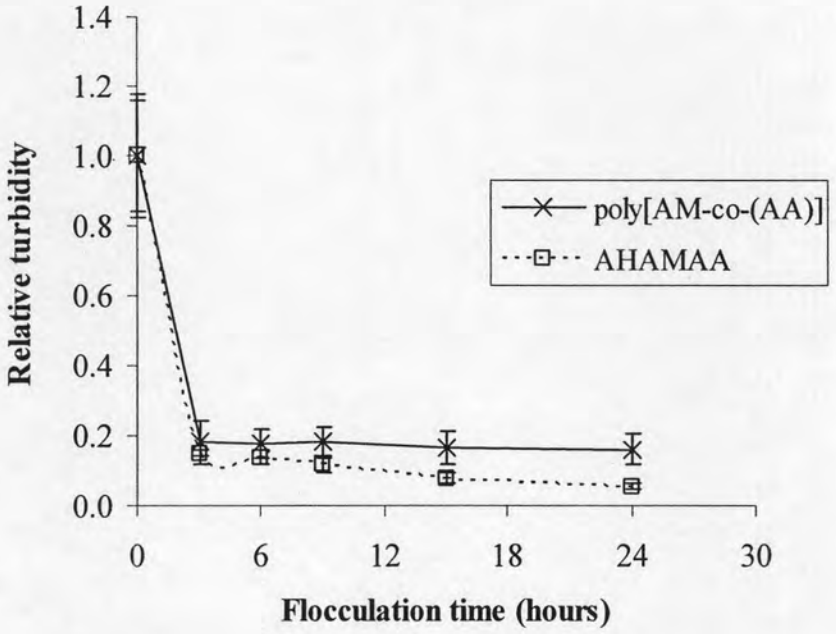


**Figure 4.30** Effect of the flocculation time on the relative turbidity of the kaolin suspension by the poly[AM-*co*-(AA)] and AHAMAA synthesized with $4x10^{-3}$ mol AA, $2.3x10^{-4}$ mol N-MBA, $1.6x10^{-4}$ mol APS, $12x10^{-4}$ mol TEMED, 250 rpm, at 45 °C and 1 h polymerization time

From this experiment, the kaolin suspension (0.1 % wt) was used a model for the turbid wastewater. The AHAMAA and poly[AM-*co*-(AA)] which are classified as organic/inorganic coagulant and flocculant, respectively, were used in a turbidity removal of the synthetic wastewater. The relative turbidity in Figure 4.30 was decreased when the flocculation time increased for AHAMAA from 3 to 24 h. The longer flocculation time in AHAMAA allowed the better reduction in turbidity up to 95%. Unlike the case of poly[AM-*co*-(AA)], the relative turbidity values were independent of flocculation time when the flocculation time was longer than 3 h. Comparing the turbidity removal efficiency, the treated synthetic turbid wastewater

treated with the AHAMAA become clearer or less turbid, i.e., the AHAMAA has the high turbidity removal efficiency than that obtained from poly[AM-*co*-(AA)] treatment. Based on the bridging flocculation mechanism and charge effect [13], the flocculation in the poly[AM-*co*-(AA)] could possibly take place via a bridging flocculation mechanism whereas the flocculation of the AHAMAA occurred by both of the charge effect and bridging flocculation. Bridging flocculation occurs because the segments of polymer chain were adsorbed on the kaolin particles and linked the particles together. For the charge effect, the charges were produced from adsorption of the cationic part (aluminium ion) of AHAMAA and the negative charge of kaolin particles [53].

Moreover, Figure 4.31 also demonstrates that the kaolin flocs formed by poly[AM-*co*-(AA)] were looser (Figure 4.31 a), whereas the AHAMAA had the dense flocs (Figure 4.31 b). From these results, AHAMAA can be thus appropriate to be used as a flocculant in turbid wastewater treatment.

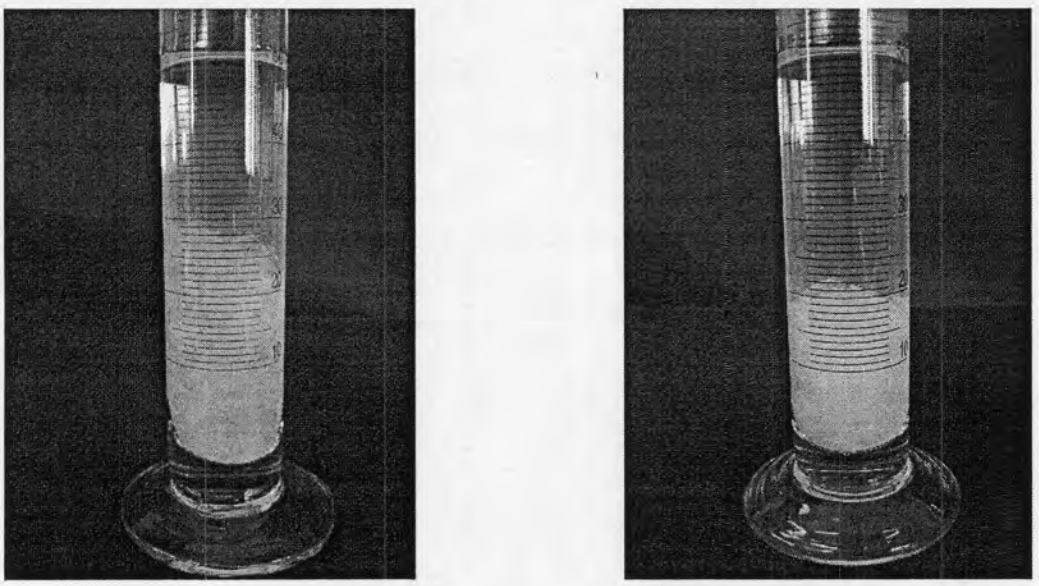

(a) (b)

**Figure 4.31** The flocs formed of (a) poly[AM-*co*-(AA)] and (b) AHAMAA

**4.9 Most possible mechanism of APS/TEMED initiated polymerization of poly[AM-*co*-(AA)] and AHAMAA**

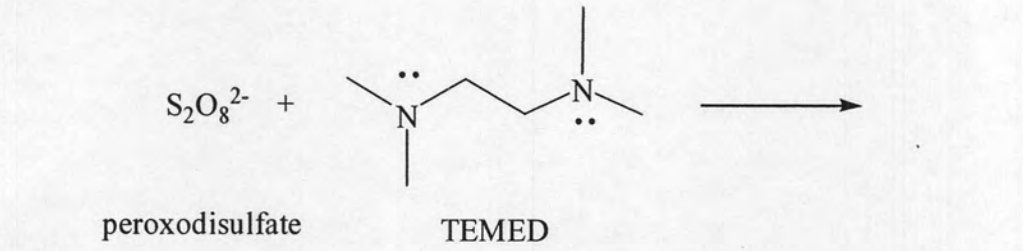


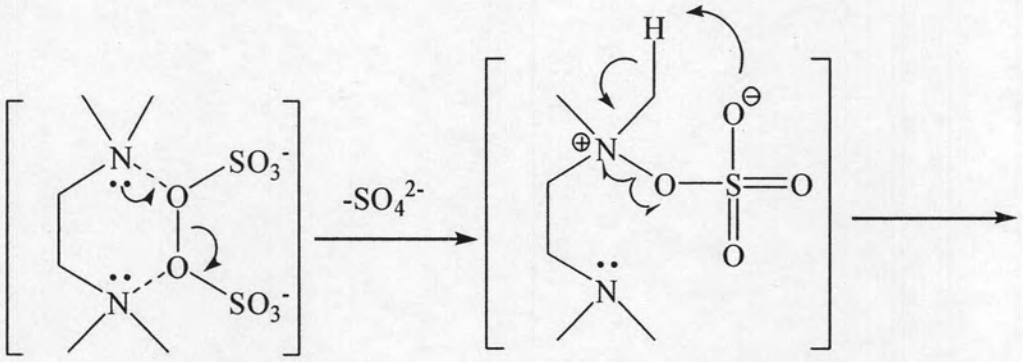


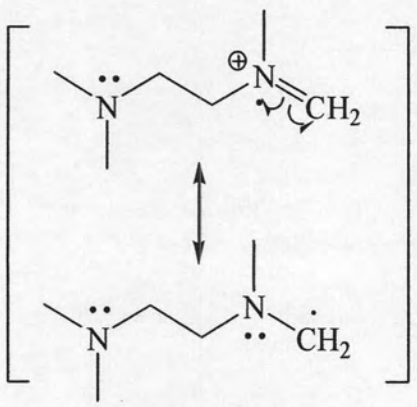


TEMED radical, [I]

+ $HSO_4^{\cdot}$

bisulfate radical

$H_2O$

$SO_4^{2-}$ + $^{\cdot}OH$

hydroxyl radical, [II]

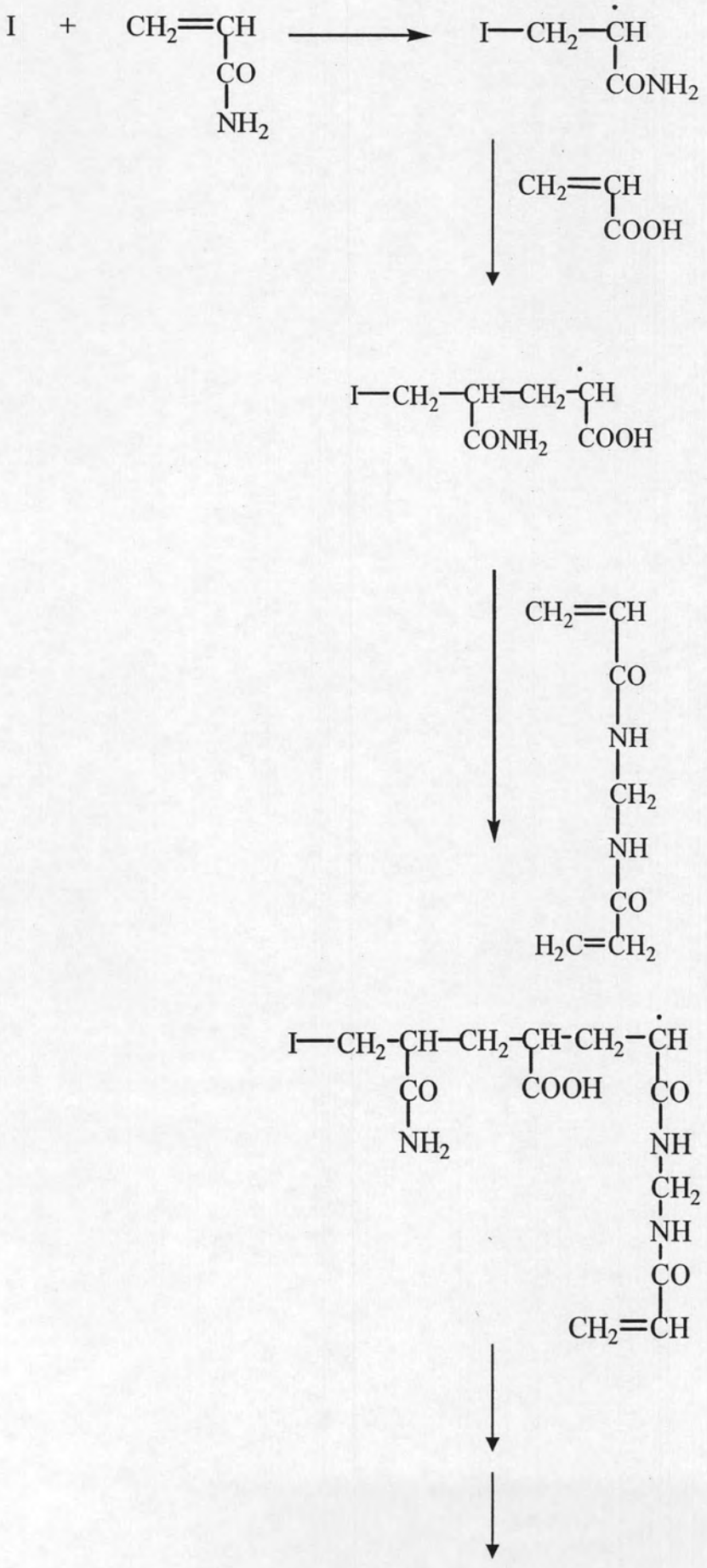

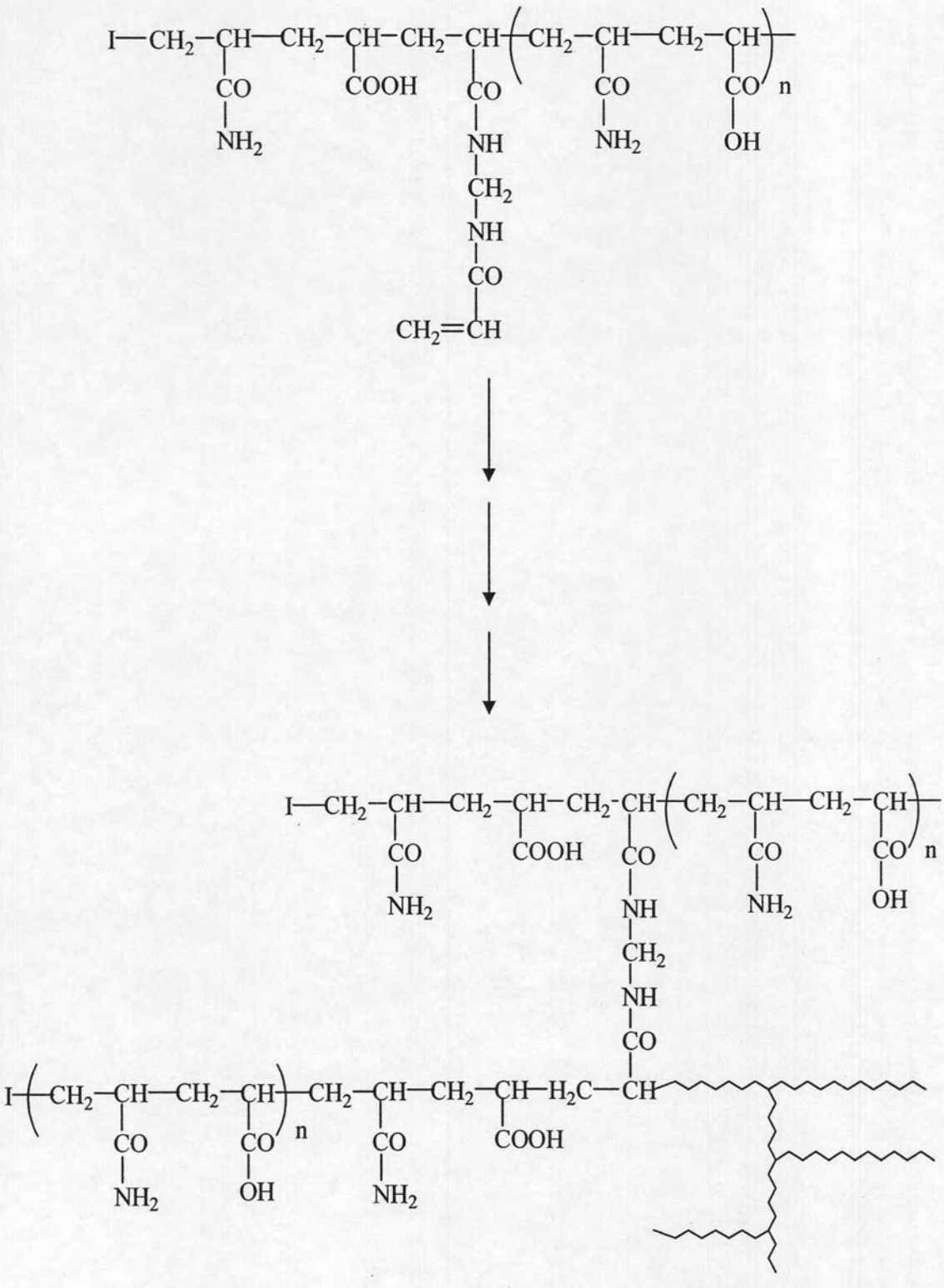

**(a)**

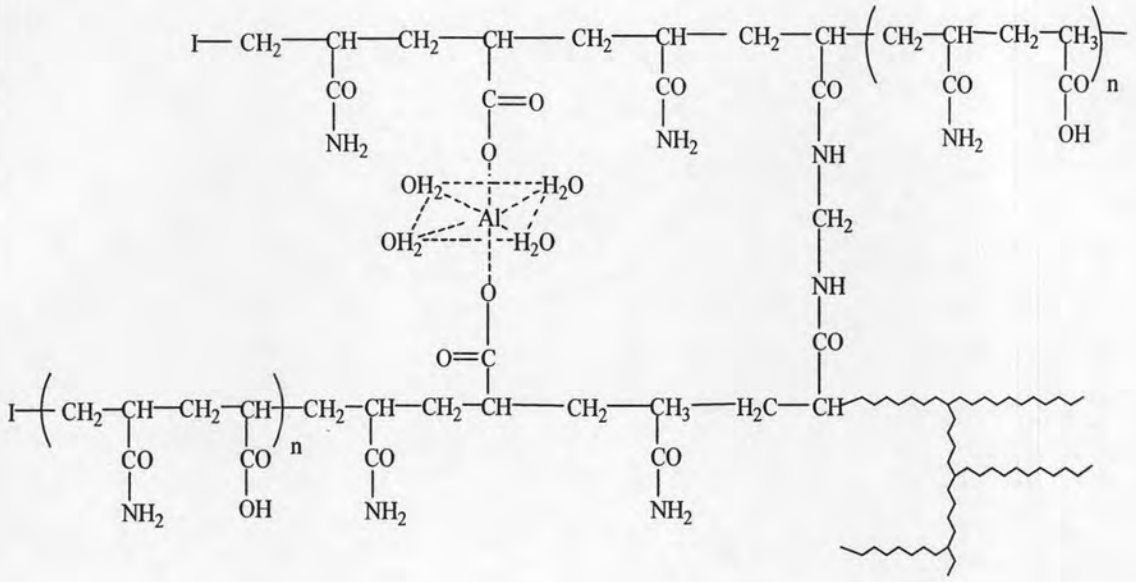

**(b)**

**Scheme 4.2** Most possible mechanism of APS/TEMED initiated polymerization of (a) poly[AM-*co*-(AA)] and (b) AHAMAA [41, 54, 55]

From the mechanism, the redox initiation of APS and TEMED in poly[AM-*co*-(AA)] system (Scheme 4.2 a) produces two radicals (hydroxyl radical and TEMED radical) which resulted in the high polymerization efficiency. This could be one reason attributed to the very high water absorption.

In the polymerization, the first step is a reaction between APS and TEMED in which the TEMED molecule is left with an unpaired electron. The activated TEMED molecule can combine with a monomer. The unpaired electron is transferred to the monomer unit, so that it in turn becomes reactive. Another monomer can be attached and activated in the same way. During the polymerization, N-MBA molecule can be incorporated into two chains simultaneously and forms a chemical crosslink between them. As a result the copolymer grows into a three dimensional network. For the OH

radical, a similar polymerization route to the TEMED radical could take place. Between them, the relative concentrations of APS and TEMED shall determine each individual contribution to superabsorbent molecular structure and the degree of water absorption, i.e., the chain length and crosslink density of the polymer.

In the case of AHAMAA (Scheme 4.2 b), the polymer-metal complex is composed of the synthetic polymer and aluminium ions. The aluminium ions are bound to the polymer ligand by a coordinate bond with oxygen atom of the carboxylate anion in one polymer chain and likewise the other chain. This type of crosslinking reaction between the two polymer chains via the aluminium ion of the $Al(OH)_3$, leading to many more crosslinking sites in the polymer chains. This could be one reason attributed to the low water absorption due to high rigidity of the polymer chain.